Master's thesis

NTNU
Norwegian University of Science and Technology
Faculty of Engineering
Department of Energy and Process Engineering

Daniel Andreas Monsen Gløsen

Experimental Studies of Carbonated Injection Water

Master's thesis in Energy and Environmental Engineering
Supervisor: Even Solbraa
June 2021

NTNU
Norwegian University of Science and Technology

equinor

Daniel Andreas Monsen Gløsen

Experimental Studies of Carbonated Injection Water

Master's thesis in Energy and Environmental Engineering
Supervisor: Even Solbraa
June 2021

Norwegian University of Science and Technology
Faculty of Engineering
Department of Energy and Process Engineering

NTNU
Norwegian University of
Science and Technology

Preface

This master's thesis is written at the Norwegian University of Science and Technology in collaboration with Equinor. In this thesis, experimental results and simulations regarding mixing of carbonated water is presented and discussed. Carbonated water can be used as a carbon storage method when injected into the ground.

I am grateful for the guidance I have received from my supervisor Even Solbraa and the collaboration with the rig operators Monica Engen, Staale Førre Jensen and Jan Terje Skjetne who have provided great assistance despite delays and lockdowns at both NTNU and Equinor.

Thanks also to Emil Høgli for his work done prior to this thesis and to Bengt Olav Neraas for inspiration and input.

Abstract

Oil and gas production is the largest contributor to Norway's total greenhouse gas emissions, meaning that there is a great potential for emission cuts. This can be solved by reducing production, but as long as there is a demand for fossil fuels, one must look for solutions that can make production as environmentally friendly as possible. CO_2 can be captured directly from the flue gas on offshore platforms using available carbon capture technology. This carbon dioxide can be used in other industries or stored underground, but transporting pure CO_2 is a challenge.

Carbonized water injection is a promising method for both enhanced oil recovery and carbon storage. Oil platforms use water injection to maintain the pressure in oil reservoirs so that more oil can be extracted from each well. By dissolving the trapped CO_2 in the injection water, the emissions can be reduced without large investment costs.

This master's thesis presents models for the solubility of CO_2 in water, as well as for kinetics in bubble flow. These models have been used to develop simulation models using software such as MATLAB and HYSYS, and the simulations have been compared to experimental data from Equinor.

Experiments have been executed by Equinor with a specially designed rig for carbonation of water. At 20 bar pressure and ambient temperature, water and gaseous CO_2 were mixed in pipes of different lengths and at different flow rates. The density of the mixture is measured at the end of the tube to tell how well the CO_2 has dissolved.

The results from the experiments show that it is challenging to control the dissolution of CO_2 in water. With a short pipe length for mixing, almost nothing is dissolved. With longer pipes, there is an increase in density, which indicates that there will be dissolved CO_2 if the residence time in the pipe is long enough. At a lower water flow rate, there is longer residence time, but less turbulence. These two opposing factors both play in favor of better dissolution. It looks like there is an optimal point where the flow rate is high enough to get good mixing by turbulence and low enough to have a long residence time in the pipe.

In a real full-scale system, you want to be sure that the carbonated water only contains dissolved CO_2, not CO_2 in a gaseous phase. The challenges in the experiments suggest staying at a CO_2 level well below the saturation value. Still, it is wanted to store as much CO_2 as possible per liter of water. The solubility of CO_2 increases with increasing pressure up to around the critical pressure where the increase in solubility flattens out. With increased pressure, compressor work also increases. Therefore, it seems that mixing CO_2 and water at a pressure below the critical pressure of CO_2 gives the best efficiency, because the benefit of increased solubility is greater than the disadvantage of higher energy requirements.

Norwegian summary

Olje- og gassproduksjon er den største bidgragsyteren til Norges totale klimagassutslipp. Det betyr at det er et stort potensiale for utslippskutt. Dette kan løses ved å redusere produksjonen, men så lenge det er etterspørsel etter fossile brensler må man se etter løsninger som kan gjøre produksjonen så miljøvennlig som mulig. CO_2 kan fanges direkte fra utslippspunktet på offshore-plattformer ved hjelp av tilgjengelig karbonfangstteknologi. Denne karbondioksiden kan utnyttes i annen industri eller lagres under bakken, men å transportere ren CO_2 er en utfordring.

Karbonisert vanninjeksjon er en lovende metode for både økt oljeutvinning og karbonlagring. Oljeplattformer bruker vanninjeksjon for å holde trykket oppe i oljereservoarene, slik at man kan hente ut mer olje fra hver brønn. Ved å oppløse fanget CO_2 i injeksjonsvannet, kan man redusere utslippene uten store investeringskostnader.

I denne masteroppgaven presenteres modeller for løselighet av CO_2 i vann, samt for kinetikk i boblestrøm. Dette har blitt brukt til å utvikle simuleringsmodeller ved hjelp av programvare som MATLAB og HYSYS, og disse simuleringene har blitt sammenlignet med eksperimentelle data fra Equinor.

Forsøk har blitt gjort av Equinor med en spesialdesignet rigg for karbonisering av vann. Ved 20 bars trykk og romtemperatur ble vann og CO_2gass blandet sammen i rør med forskjellige lengder og ved forskjellige strømningsrater. Tettheten til blandingen måles ved enden av røret for å fortelle hvor godt innblandet CO_2-en er.

Resultatene fra forsøkene viser at det er utfordrende å løse opp CO_2 i vann kontrollert. Med kort rørlengde for miksing blir nesten ingenting løst inn. Med lengre rør kan man se en økning i tetthet, noe som indikerer at det vil skje en oppløsning av CO_2 dersom oppholdstiden i røret er lang nok. Ved lavere vannrate får man lengre oppholdstid, men mindre turbulens. Disse to motvirkende faktorene spiller begge i favør av bedre oppløsning. Det ser ut til at det finnes et optimalt punkt der strømningsraten er høy nok til å få god miksing ved turbulens, og lav nok til å få lang oppholdstid i røret.

I et ekte fullskalasystem ønsker man å være sikker på at det karboniserte vannet kun inneholder CO_2 løst i vann, ikke CO_2 i gassfase. Utfordringene i forsøkene tyder på at man bør holde seg på et CO_2-nivå langt under metningsverdien. Likevel ønsker man å få lagret så mye CO_2 som mulig per liter vann. Løseligheten av CO_2 øker ved økende trykk opp til rundt det kritiske trykket hvor økningen i løselighet flater ut. Med økt trykk øker også kompressorarbeidet. Derfor virker det som at å blande CO_2 og vann ved et trykk i underkant av det kritiske trykket til CO_2 gir best effektivitet, fordi gevinsten av økt løselighet er større enn ulempen av høyere energibehov.

Table of Contents

List of Figures vi

List of Tables vi

Nomenclature viii

1 Introduction 1

2 Background 2

3 Theory 3

3.1 Behaviour of CO_2 . . . 3

3.2 CO_2 solubility in water . . . 4

3.2.1 Henry's law . . . 5

3.2.2 Other models . . . 6

3.3 Mass transfer through diffusion . . . 8

3.3.1 Diffusion models . . . 8

3.3.2 Mass transfer coefficients and diffusivity . . . 9

3.4 Gas-liquid flow behaviour . . . 12

3.4.1 Bubble size . . . 12

3.4.2 Mixing . . . 14

3.5 Upscaling . . . 17

4 Method 18

4.1 Procedure of simulation . . . 18

4.1.1 MATLAB . . . 18

4.1.2 HYSYS . . . 20

4.2 Procedure of experiments . . . 21

5 Experimental rig 23

5.1 Description . . . 23
5.2 Experimental uncertainty . . . 29

6 Results **30**
6.1 Comparison of solubility models . . . 30
6.2 Rig results . . . 31
6.3 Simulation results . . . 33

7 Discussion **39**
7.1 HYSYS simulations . . . 39
7.2 Comparison of MATLAB simulations and experiments . . . 40
7.3 Upscaling . . . 41

8 Further work **43**

9 Conclusion **44**

Bibliography **45**

Appendix **49**
A MATLAB code . . . 49
A.1 CW . . . 49
A.2 global_param . . . 51
A.3 masstrans_coeffs . . . 52
A.4 PlotLoop . . . 53
A.5 Re_k_plot . . . 56
A.6 SolComp . . . 57
B P&ID of CW rig . . . 59
C Master's agreement . . . 60

List of Figures

1 CO_2 phase diagram . . . 3
2 P-T diagram with solubility isopleths . . . 7
3 Flow patterns . . . 13
4 Flow pattern maps . . . 14
5 Tee mixer . . . 15
6 Model of experimental rig . . . 18
7 HYSYS case study system . . . 21
8 P&ID . . . 23
9 Picture of CW rig . . . 24
10 New mixing element . . . 25
11 Pictures of rig with hose . . . 25
12 Controlling and monitoring screen of CW rig . . . 29
13 Comparison of solubility models . . . 30
14 HYSYS density results . . . 31
15 Mass transfer coefficients by Re . . . 33
16 Density with different mass transfer coefficients . . . 34
17 Rig simulation 1 . . . 35
18 Rig simulation 2 . . . 35
19 Rig simulation 3 . . . 36
20 Rig simulation 4 . . . 36
21 Rig simulation 5 . . . 37
22 HYSYS energy simulation . . . 37

List of Tables

1 Henry's constant . . . 5
2 Henry's law data . . . 6

3 CO_2 solubility 8

4 Diffusion coefficients 11

5 Component list 26

6 Fugacity coefficients 30

7 Rig results 32

8 HYSYS energy simulation results 38

9 Scale-up case 42

Nomenclature

c_A	Concentration of species A in water	$mol\ m^{-3}$
k_H	Temperature dependant Henry's law constant	$mol\ kg^{-1}\ bar^{-1}$
k_H^0	Henry's law constant at 298.15 K	$mol\ kg^{-1}\ bar^{-1}$
$\frac{d(ln(k_H))}{d(1/T)}$	Temperature dependence constant	K
H	Henry's constant	bar
x_A	Solubility of species A in water	$mol_A\ mol_{\mathrm{H_2O}}^{-1}$
p_A	Partial pressure of species A	bar
f	Fugacity	bar
Φ	Fugacity coefficient	–
j_A	Diffusive mass flux of A	$kg\ s^{-1}\ m^2$
ω_A	Mass fraction of A	–
V	Volume	m^3
A	Area	m^2
ρ	Density	$kg\ m^{-3}$
k	Mass transfer coefficient	$m\ s^{-1}$
D_{AB}	Diffusion coefficient	$m^2\ s^{-1}$
ν	Kinematic viscosity	$m^2\ s^{-1}$
J_l	Liquid superficial velocity	$m\ s^{-1}$
U_{rel}	Relative velocity of bubbles	$m\ s^{-1}$
d	Diameter	m
Sh	Sherwood number	–
Re	Reynolds number	–
v	Velocity	$m\ s^{-1}$
$\dot{V}$	Volume flow	$m^3\ s^{-1}$
A_{pipe}	Internal cross-sectional area of the pipe	$m^2\ s^{-1}$
μ	Dynamic viscosity	$kg\ m^{-1}\ s^{-1}$
Sc	Schmidt number	–

A_b	Area of one bubble	m^2
$A_{interface}$	Area of the interface between gas and liquid	m^2
N_b	Number of bubbles	$-$
V_{CO_2}	Volume of CO_2 gas	m^3
V_b	Volume of one bubble	m^3
$\dot{V}$	Volume flow	$m^3\ s^{-1}$
L_{pipe}	Length of pipe	m
T_{in}	Inlet temperature	$°C$
P_{in}	Inlet pressure	bar
M	Molar mass	$kg\ mol^{-1}$
$\dot{m}$	Mass flow	$kg\ s^{-1}$
R	Ideal gas constant	$J\ mol^{-1}\ K^{-1}$

1 Introduction

Norway has signed the Paris agreement, which is an international treaty with the goal of limiting the global temperature rise of the planet to 1.5 °C above pre-industrial level. To achieve this, the countries that have signed the agreement are obliged to lower their greenhouse gas emissions. Carbon dioxide is one of the most important greenhouse gases, and in Norway's plan for their national contribution they, include carbon capture and storage as one way to lower the emissions (NDC Registry, 2020).

Recent statistics from Statistics Norway reveal that Norway had a total emission of 50.0 million tonnes of CO_2 equivalents in 2020, meaning that we did not reach the goal of 48.6 million (Norum and Solvang, 2021; Røhnebæk, 2021). Oil and gas extraction still keeps the top spot for emissions, with 13.3 million tCO_2e. This should be a motivation for improving the energy production sector so that it becomes more environmentally friendly. As long as there is a need for fossil fuels, we must strive to lower these emissions as much as possible.

Carbon capture and storage (CCS) technologies have been developed over the last few years to a level at which it is starting to become economical, and big companies are able to use them. The Norwegian government launched the CCS project Longship in 2020, which the Minister of Petroleum and Energy claims to be "the greatest climate project in Norwegian industry ever" (Regjeringen.no).

One particular CCS method is carbonated water injection (CWI). At some oil reservoirs, water is injected to maintain the pressure level. The principle of CWI is to mix CO_2 into this injection water so that CO_2 is stored inside the reservoir. Even though the concept is simple, it is not a widely used CCS method today.

This thesis aims to study the behaviour of carbonated water at intermediate pressure levels and investigate how this can be applied to a full-scale situation. The focus will be on the kinetics of CO_2 gas bubble flow in liquid water. The objective is to find a model that can describe a small-scale CW system and discuss how to design a full-scale system. This will be done through tests using an experimental rig that mixes CO_2 and water and measures the mix density, and by comparing the results with calculations from simulation and programming software. The problem description as written in the Master's agreement is available in Appendix C.

2 Background

The emissions connected to fossil fuel production are and have been high for a long time. Therefore, international treaties and national restrictions have forced companies to lower their emissions. At the same time, both the demand for fossil fuel and the economic aspect makes it impossible to suddenly make a massive cut in production. Therefore, there is a need to find ways of lowering emissions while keeping high production. This can be done with carbon capture and storage.

There are several ways of storing carbon dioxide. Firstly, it has to be separated from the flue gas, which can be done with technology already available on the market for full-scale applications. Aker Solutions' Just Catch system based on amine absorption is one of the market leaders in carbon capture, which can separate out almost pure CO_2. The requirement for CCS is that it has to be transported to someplace where it will not affect the atmosphere.

Storing CO_2 underground under high pressure keeps the CO_2 away from the atmosphere, but may require boring new suitable storage areas. Carbonated water injection is another alternative. CWI stores CO_2 underground, similarly to what was mentioned above, but also serves a purpose as injection water. Water injection (WI) is the process of injecting water into an oil reservoir in order to increase the pressure and direct the oil towards the well, enhancing the oil recovery. WI can greatly impact how much of the oil in the reservoir that is possible to retrieve. An example is the Ekofisk field which has increased its recovery factor from 17% to above 50% after introducing WI (Norwegian Petroleum Directorate, 2020). By dissolving CO_2 into the injection water at high pressure, large volumes of CO_2 can be transported using already installed pumps and pipes. Studies have shown that CWI may be even more beneficial than regular WI because CO_2 reacts with the petroleum and generates better flow (Sohrabi et al., 2011).

Equinor is Norway's largest power company and has oil and gas production as their most important business. They have a lot of offshore petroleum industry, where they use WI as an enhanced oil recovery (EOR) method today. If it is possible to capture and mix CO_2 in to the injection water easily, it will make their offshore platforms the perfect place to use CWI. This way, there would be no need for making a separate and designated injection well for the CWI in addition to the injection well for WI. This could save much money, both in capital expenses and in CO_2 emission fees.

Water can hold a given amount of dissolved CO_2 at a given pressure at equilibrium, but the difficult question is relating equilibrium theory and ideal cases to a real case pipe flow. This must be done carefully in order to know how to store as much CO_2 as possible at industrial scale. Equinor has provided a typical case to study in this thesis: starting at 1 bar, an annual emission of 180 000 tonnes CO_2 is to be converted into carbonated water at 200 bar. Making of the carbonated water could happen at either low pressure, intermediate pressure, or high pressure. Using Equinor's experimental CW rig, tests at 20 bar pressure can help to establish a model for the behaviour at intermediate pressure.

3 Theory

The calculations in this thesis are based on theory and equations presented in Emil Høgli's master thesis, (Høgli, 2020), in addition to other scientific works. In order to make a simulator for an experimental carbonated water system, it is important to have a rigid model for the transfer of CO_2 into the water phase. Therefore, information about solubility, mass transfer properties and bubble geometry is needed.

3.1 Behaviour of CO_2

Carbon dioxide is a chemical compound with molecules consisting of one carbon atom and two oxygen atoms. CO_2 has many properties that can be used to our benefit in different industrial processes. It also has some drawbacks, the most infamous of which is that it works as a greenhouse gas. One of the benefits is however that it is soluble in water, which is something that can be utilized for CO_2 storage.

When CO_2 dissolves in water, some of it reacts to form a small amount (around 0.2%) of carbonic acid (Pedersen, 2017). This makes the solution weakly acidic. The rest of the CO_2 remains as dissolved gas in an aqueous phase (Knoche, 1980). This molecular diffusion mechanism results in an increase of density (Ahmadi et al., 2020), a concept that will be discussed further in Section 3.4.

Carbonated water injection happens at high pressure. Therefore, it is important to have in mind the behaviour of CO_2 at different pressure and temperature levels. A CO_2 phase diagram can be seen in Fig. 1. The critical point of CO_2 is at a temperature of 31.1 °C and a pressure of 73.8 bar. CO_2 does not have the same behaviour in supercritical state as for as a gas, which is a reason why many models of solubility and mass transfer are very different above and below the critical pressure.

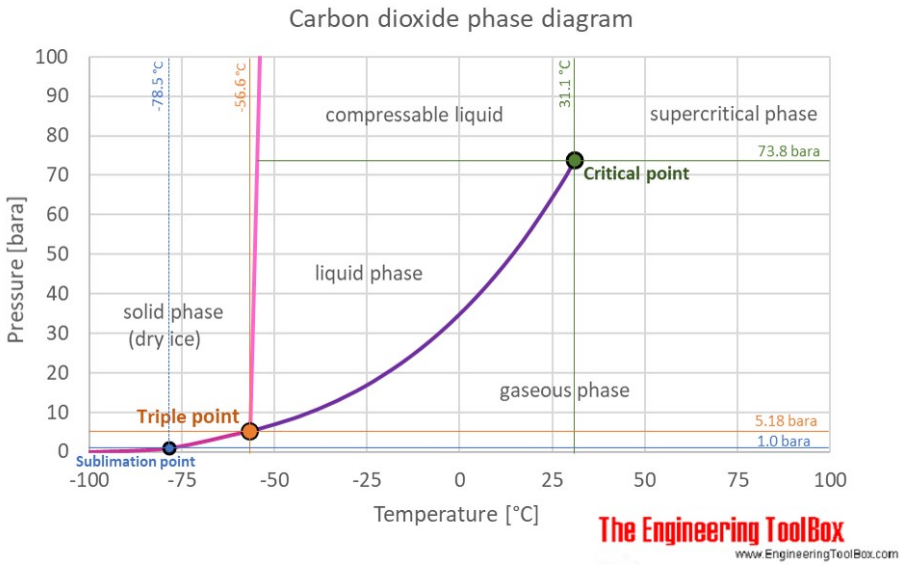

Figure 1: CO_2 phase diagram

3.2 CO_2 solubility in water

CO_2 is soluble in water, meaning that it can be a part of the aqueous phase instead of being in gaseous phase. As with all soluble substances, water can dissolve them up until a certain amount – the saturation point. This point is dependant on both pressure and temperature, as well as the amount of other substances present in the water. Sea water can not contain as much CO_2 as fresh water, because of the already dissolved salt. At the saturation point, the water cannot dissolve any more CO_2, and gas bubbles will appear. Higher pressure increases the amount of CO_2 we can add before we reach saturation.

CO_2 is what makes the bubbles in carbonated beverages such as soda or champagne. An unopened soda bottle is under pressure and at equilibrium. At equilibrium, the soda usually contains no visible bubbles, because the liquid is saturated and the gas has risen to the top of the bottle, building up pressure. When the bottle is opened, bubbles become visible as they rise from the bottom of the bottle. This is because opening the cap reduces the pressure, and thus also reduces the maximum solubility of the liquid. When the pressure above the liquid is reduced to atmospheric pressure, the amount of CO_2 that can be dissolved in the liquid reduces according to Henry's law, Eq. (1).

Pressure and temperature play a great role in the calculations of the solubility for a real system. These parameters have to be tuned in order to achieve the highest possible concentration of CO_2 in the water. As mentioned, higher pressure gives higher solubility, according to Henry's law. Therefore, it will be beneficial to mix together water and CO_2 at high pressure to dissolve as much as possible. The pressure level should not exceed the pressure level where it will be stored, or else the water will no longer contain the same amount of dissolved CO_2. At normal temperatures CO_2 is a gas at atmospheric pressure, and therefore it needs compression to get to higher pressure levels. When dissolved into the water, so that there is only liquid present, a pump can be used instead of a compressor, opening for higher pressure factors and possibly less energy consumption.

Mixing at low pressure requires little energy, but solubility is also low. At high pressure, solubility is high, but the work needed is also high. Finding the optimal pressure levels and compressor configuration with respect to power consumption is therefore one of the big challenges.

The solubility considerations here assume equilibrium. However, it's not given that equilibrium is easily achieved. The rate at which a CO_2-water-system gets to equilibrium is determined by its kinetic factors, discussed in Section 3.3. At the same time, we do not actually want to achieve equilibrium in the carbonated injection water, as that means that there will be gas present in the system. The goal is rather to reach a point where a lot of CO_2 has been dissolved, but still under-saturated so that all CO_2 can remain dissolved.

A rise in pressure generally increases the solubility, because one phase of carbonated water is more dense than two phases of gas and liquid, taking up less space. This is true as long as temperature stays constant. However, an increase in temperature gives either lower or higher solubility, depending on the pressure level. Bisweswar et al. (2019) states that this difference happens at $P = 30$ MPa, where $P > 30$ MPa causes solubility to increase with

increasing temperature, while $P < 30$ MPa causes solubility to decrease with increasing temperature. In addition, viscosity can be significantly reduced from rising temperatures (Bisweswar et al., 2019).

3.2.1 Henry's law

Henry's law, Eq. (1), can be applied on mass transfer of species A from a gas phase into a liquid, where A is weakly soluble (Incropera et al., 2013). It relates the solubility of A in the liquid, x_A, to the partial pressure of A outside the liquid p_A. $x_A(0)$ and $p_A(0)$ are the solubility and partial pressure at zero distance from the other phase, i.e. at the interface.

$$x_A(0) = \frac{p_A(0)}{H} \tag{1}$$

H (bar) is the temperature dependant Henry's constant which can be found in Table 1. It also varies with pressure, but this dependence can be neglected if the pressure is below 5 bar. This thesis looks at pressure levels way above that limit, which means that Henry's law cannot be trusted when the gases it is applied to are non-ideal. Also, it must be determined whether CO_2 is categorized as weakly soluble, as it is a condition for using the formula. At high pressure, CO_2 is much more soluble than at low pressure, so that may cause Henry's law to be an inaccurate way of calculating the solubility.

Table 1: Henry's constant for CO_2 in water at moderate pressure

$\boldsymbol{H = p_{A,i}/x_{A,i}}$ $\boldsymbol{(bar)}$	
T (K)	CO_2
273	710
280	960
290	1300
300	1730
310	2175
320	2650
323	2870

Source: Incropera et al. (2013)

Dalton's law of partial pressures tells that the pressure p of a gas is the sum of the partial pressures of the i species in the gas (Incropera et al., 2013):

$$p = \sum_i p_i \tag{2}$$

If CO_2 is the only gas in the gas phase, then the partial pressure of CO_2 will naturally be the same as the total gas pressure. With this assumption, we can also assume that the gas phase is uniform, i.e. $p_A(0) = p_A = p$.

According to Sander (2015), there are several variants of Henry's law constants described by either molar concentration, molality, partial pressure etc. It is therefore important

to be consistent when choosing and using a set of coefficients and their corresponding formulas. There are also many symbols that look very similar but represent different types of Henry's law constants. In general, there are many symbols that look alike, also in this thesis. Therefore the Nomenclature should be used when in doubt.

H has unit $bars$, but Sander (2018) uses a Henry's law constant they call k_H with unit $mol\ kg^{-1}\ bar^{-1}$. This latter type of constant may be beneficial to use in a model that numerically looks at the number of moles transferred to a given mass of water at a given pressure. The formula for calculating k_H is presented in Eq. (3) (Sander, 2018) with the use of temperature dependence constants found in Table 2.

$$k_H(T) = k_H^0 e^{\frac{d(ln(k_H))}{d(1/T)}(\frac{1}{T} - \frac{1}{298.15K})} \tag{3}$$

Where
k_H^0 – Henry's law constant at 298.15 K ($mol\ kg^{-1}\ bar^{-1}$)
$\frac{d(ln(k_H))}{d(1/T)}$ – Temperature dependence constant (K)

Table 2: Henry's law data for CO_2 solubility in water.

k_H^0	.035	.034	.045	.035	.034	.034	.034	.031	.034	.034	.034	.032	.035	.034	.034	.034	.034
$\frac{d(ln\ k_H)}{d(1/T)}$	2400	2600	N/A	2300	2400	2400	2400	2400	2400	N/A	N/A	2400	2400	2400	2400	2700	2400

Source: Sander (2018)

3.2.2 Other models

Diamond and Akinfiev (2003) presented a P-T diagram of the solubility of CO_2 in water, seen in Fig. 2. Reading off Fig. 2b at 18 °C, we can expect a solubility of 0.75 mol% at 10 bar, 1.3 mol% at 20 bar and 1.8 mol% at 30 bar, while at 30 °C, there is a solubility of 0.50 mol% at 10 bar, 0.98 mol% at 20 bar, 1.35 mol% at 30 bar, 1.70 mol% at 40 bar and 1.95 mol% at 50 bar.

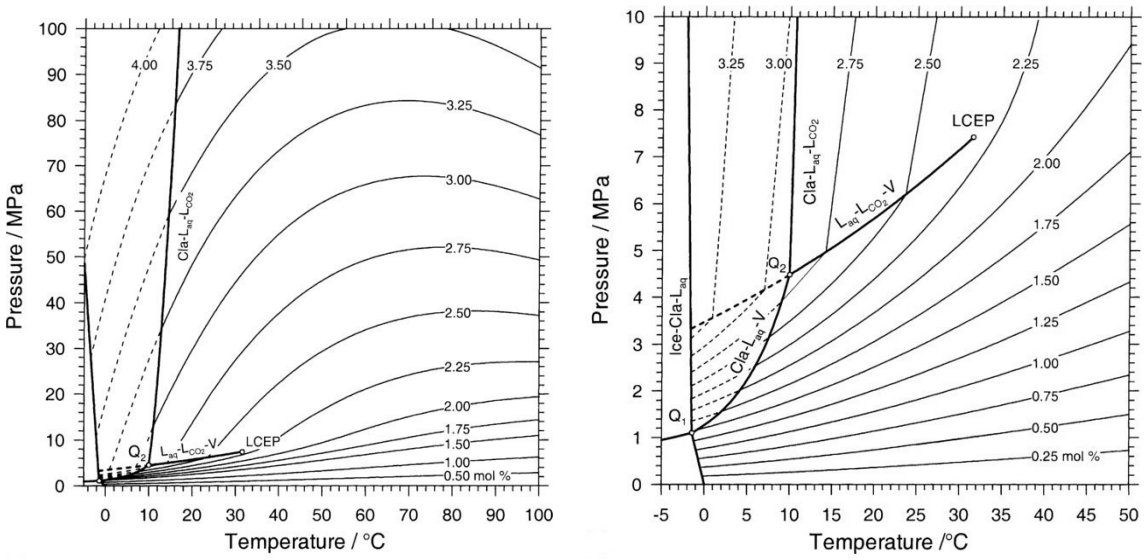

(a) Entire P–T region of model validity

(b) Details of low-P, low-T region.

Figure 2: Pressure-temperature diagram with solubility isopleths from 0.25 mol% to 4 mol%.

Source: Diamond and Akinfiev (2003)

Crovetto (1991) lists a great number of Henry's law constants, but none in a similar temperature and pressure range as that of this project, which is around 18 °C and 10 to 30 bar. This group was not included because "*This group is very difficult to evaluate because for some experimental* P *and* T *conditions carbon dioxide is very near its critical point*".

Duan and Sun (2003) is a comprehensive paper that introduces an improved model for CO_2 solubility in water for a wide range of pressure, temperature and salinity. The model is implemented in the program *NeqSim* which is a non-equilibrium simulator developed by Even Solbraa and is available from Github. Duan and Sun also includes a table of solubilities from some selected temperature and pressure levels, of which an excerpt is seen in Table 3.

Since Henry's law assumes ideal gas, it will be more and more inaccurate as the pressure increases. However, instead of using the pressure, we might be able to use the fugacity. Fugacity is an effective pressure which can replace the true pressure to account for gas imperfections so that the pressure dependence of the Gibbs energy is still valid (Atkins and De Paula, 2006). Fugacity, f, has the same unit as pressure, and plays the same role in the general case as pressure does in the ideal case (Moran et al., 2012). By multiplying the pressure with a fugacity coefficient, ϕ, a more accurate model for the solubility could be achieved by using Henry's law with this adjustment.

A comparison of these models is done in Comparison of solubility models.

Table 3: Calculated CO_2 solubility in water for T=303.15 K

P (bar)	CO_2 solubility (mol/kg water)	CO_2 solubility 4 m salinity (mol/kg water)
1	0.0286	0.0147
5	0.1442	0.0703
10	0.2809	0.1339
50	1.0811	0.4945
100	1.3611	0.6189
200	1.4889	0.6849
300	1.5989	0.7515
400	1.7005	0.8200
500	1.7965	0.8907

Source: Duan and Sun (2003)

3.3 Mass transfer through diffusion

As discussed in Section 3.2, water can at a given pressure and temperature hold a certain amount of CO_2. However, this maximum amount is achieved at equilibrium, but equilibrium is not always possible to achieve. Ahmadi et al. (2020) found in their experiments that the time to reach CO_2-H_2O-equilibrium at 298 K took over 8 hours at 20 bar, and 4.5 hours at 57 bar.

If mixing happens at low pressure, then the carbonated water needs to be pumped up to injection pressure between mixing and injection. Having large bubbles in the flow may cause problems for the pump (Hydraulic Institute, 2015), so it is preferred to keep the CO_2 level way below saturation. To assure that there is no gas present when our mixed fluid goes through the pump, we have to have a sufficient mixing. That may require a long mixing pipe or an advanced mixing element. If the amount of CO_2 is smaller than the maximum solubility, all of it will dissolve after long time, i.e. after going through a long enough pipe. However, we want the equipment cost to be as low as possible as well as a small physical footprint, meaning that the pipe should not be longer than necessary.

Diffusion is the transfer of substance from an area of high concentration to an area of low concentration through random motion (UiO, 2020). According to Cussler (2009), diffusion can be a slow process, and if it is the slowest step in a process, it will be the limiting factor for the overall efficiency.

3.3.1 Diffusion models

The German doctor Adolf Fick (1829-1901) described the behaviour of diffusion through the relation in Eq. (4). This is called Fick's law, and is the rate equation for the transfer of a species A in a binary mixture of A and B on mass basis (Incropera et al., 2013). For this project, it can be used to find the amount of CO_2 that is transferred by diffusion per

second and square meter.

$$j_A = -\rho D_{AB} \nabla \omega_A \tag{4}$$

j_A ($kg\ s^{-1}\ m^{-2}$) is the diffusive mass flux of A and is proportional to the mix density, ρ ($kg\ m^{-3}$), and the mass fraction of A, $\omega_A = \frac{\rho_A}{\rho}$, the latter of which is the driving force Incropera et al. (2013). The diffusion coefficient D_{AB} ($m^2\ s^{-1}$) relates to how fast the diffusion takes place.

Fick's law of diffusion is the most fundamental model for diffusion, using a diffusion coefficient (Cussler, 2009). However, there is also a second type of diffusion model commonly used, which uses a mass transfer coefficient instead:

$$V \frac{dc_A}{dt} = kA[c_A(sat) - c_A] \tag{5}$$

k ($m\ s^{-1}$) is the mass transfer coefficient (not to be confused with k_H and k_H^0), c_A ($mol\ m^{-3}$) is the concentration of species A in the bulk solution, and $c_A(sat)$ is the concentration at the saturation point, i.e. at equilibrium. V (m^3) is the volume of the solution, while A (m^3) is the contact area between phases. The concentration difference is the driving force, which says something about the potential for mass transfer, while k tells how fast the mass transfer can happen, and is dependant on what kind of species that exist in the system. For instance, a system of nitrogen gas and oxygen gas has a different mass transfer coefficient than a system of liquid water and carbon dioxide gas.

Using diffusion coefficients is necessary if the goal is to be general and accurate, but in experimental cases it might be more relevant to use mass transfer coefficients (Cussler, 2009). Since this is an experimental thesis, it is the model using mass transfer coefficients, Eq. (5), that will be used. Still, diffusion coefficients are necessary in some of the mass transfer coefficient models.

3.3.2 Mass transfer coefficients and diffusivity

Since mass transfer coefficients are related to experimental and non-fundamental models, there are many different ways of estimating them, as well as a number of data available in tables. There is no general and precise way of calculating mass transfer coefficients, since they are often gathered from experimental data and vary from system to system based on the different substances present as well as on temperature, pressure, Reynolds number, geometry, etc. For this thesis, the relevant mass transfer coefficients are those that are valid for co-current bubble flow in a horizontal tube. Høgli (2020) presented a set of equations for mass transfer coefficients for different ranges of Reynolds number and different types of systems.

The mass transfer coefficient, k, can be calculated either directly as in Eqs. (6) to (8) or from the Sherwood number, as in Eq. (9). Eqs. (6) to (8) are obtained from Rzehak

(2016) and Høgli (2020), of which Eq. (6) is for small eddies, Eq. (7) for large eddies, and Eq. (8) is for laminar flow.

$$k = 1.7\frac{(\nu D_{AB})^{0.5}}{d_b}(\frac{J_l d_h}{\nu})^{0.46} \tag{6}$$

$$k = 0.71\frac{(\nu D_{AB})^{0.5}}{d_b}(\frac{J_l d_h}{\nu})^{0.69} \tag{7}$$

$$k = 1.13\frac{(\nu D_{AB})^{0.5}}{d_b}(\frac{U_{rel} d_b}{\nu})^{0.5} \tag{8}$$

$$k = \frac{ShD_{AB}}{d_{pipe}} \tag{9}$$

Where

D_{AB} – Diffusion coefficient $(m^2\ s^{-1})$
ν – Kinematic viscosity of liquid $(m^2\ s^{-1})$
J_l – Liquid superficial velocity $(m\ s^{-1})$
U_{rel} – Relative velocity of bubbles $(m\ s^{-1})$
d_h – Hydraulic diameter (m)
d_b – Bubble diameter (m)
Sh – Sherwood number $(-)$
d_{pipe} – Inner diameter of pipe (m)

D_{AB} is the diffusion coefficient of species A into species B which was presented with Fick's law in Section 3.3.1. It is dependant on temperature and pressure, and also on which substances that are involved. Cadogan et al. (2014) presents a table of diffusion coefficients for different temperatures and pressures where D_{AB} is $2.233 \cdot 10^{-9}\ m^2/s$ at 140 bar and $2.256 \cdot 10^{-9}\ m^2/s$ at 316 bar, for 25 °C. Frank et al. (1996) found that D_{AB} is $1.97 \cdot 10^{-9}\ m^2/s$ at 1 bar and 25 °C. According to Cussler (2009), CO_2 has a diffusion coefficient of $1.92 \cdot 10^{-9}\ m^2/s$ at infinite dilution in water at 25 °C. These together with other diffusion coefficients are listed in Table 4.

Ahmadi et al. (2020) did an experimental study on the diffusion coefficient of CO_2 in water, where they concluded that at a constant pressure of 58 bar the diffusion coefficient increased with increasing temperature. Also, at constant temperature of 298 K and 323 K, the coefficient increased with increasing pressure. Additionally, they noticed a substantial drop in the diffusion coefficient when there was phase alteration from gaseous to supercritical conditions.

The Sherwood number, Sh, is calculated using a relation only dependant on the liquid phase Reynolds number, Re_L, and the Schmidt number, Sc. Three different Sherwood relations are compiled by Høgli (2020):

For $1200 < Re_L < 2400$, with average error of 22.29% (Ciborowski and Rychlicki, 1971):

$$Sh = 0.00413 Re_L^{0.916} Sc^{0.5} \tag{10}$$

For $6926 < Re_L < 43282$, with average error of 7.41% (Valiorgue et al., 2011):

$$Sh = 1.76 \cdot 10^{-5} Re_L^{1.506} Sc^{0.5} \tag{11}$$

For $18000 < Re < 160000$, with deviation in $ln\frac{Sh}{Sc^{0.5}}$ of 0.19 (T.S. Kress, 1973):

$$Sh = 0.335 Re^{0.94} Sc^{0.5} \frac{d_{sm}}{d_h} \tag{12}$$

In Eq. (12), d_{sm} is the Sauter mean diameter of the bubbles, and d_h is the hydraulic diameter of the pipe flow. This particular equation is only valid for $0.254\ mm < d_{sm} < 1.27\ mm$ (Høgli, 2020). It is not specified, neither in T.S. Kress (1973) nor Høgli (2020), whether or not the Reynolds number in Eq. (12) is for the liquid phase or for the mixed flow.

In his thesis regarding gas absorption in co-current turbulent bubble flow, Lamont (1966) found that the mass transfer coefficient varied from 0.62 to 2.12 cm/min (equals $1.0 \cdot 10^{-4}$ to $3.5 \cdot 10^{-4}\ m/s$), for superficial liquid Reynolds numbers in the range of 3140–16800. The tube used in his measurements was horizontal and had a diameter of 5/8 inches.

Table 4: List of diffusion coefficients for CO_2 in water

D ($10^{-5}\ cm^2/s$)	T (°C)	Pressure	Salt content	Source
1,26	10	1 atm	0 M	Engineering ToolBox (2008)
1,45	15	1 atm	0 M	Engineering ToolBox (2008)
1,67	20	1 atm	0 M	Engineering ToolBox (2008)
1,91	25	1 atm	0 M	Engineering ToolBox (2008)
2,17	30	1 atm	0 M	Engineering ToolBox (2008)
2,47	35	1 atm	0 M	Engineering ToolBox (2008)
1,92	25	1 bar	0 M	Mostinsky (2011)
1,91	25	1 atm	0 M	Bours et al. (2008)
2,233	25	140 bar	0 M	Cadogan et al. (2014)
2,256	25	316 bar	0 M	Cadogan et al. (2014)
1,97	25	1 bar	0 M	Frank et al. (1996)
2,0	25	1 atm	0 M	App. A.8 in Incropera et al. (2013)
1,85	25	1 atm	0 M	Takemura and Matsumoto (2000)
1,5	25	1 bar	1 M	Takemura and Matsumoto (2000)
2.54	25	20.74 bar	0 M	Ahmadi et al. (2020)
2.75	25	34.54 bar	0 M	Ahmadi et al. (2020)
3.86	25	49.02 bar	0 M	Ahmadi et al. (2020)
5.01	25	57.16 bar	0 M	Ahmadi et al. (2020)
5.23	50	21.10 bar	0 M	Ahmadi et al. (2020)
5.81	50	33.99 bar	0 M	Ahmadi et al. (2020)
6.13	50	48.19 bar	0 M	Ahmadi et al. (2020)
6,30	50	58.4 bar	0 M	Ahmadi et al. (2020)

The Reynolds number, Re, is a dimensionless number that classifies whether a flow is laminar, turbulent or in a critical transition between the two. The higher the Reynolds number is, the more turbulent. For pipe flow, the flow is regarded as turbulent if $Re > 4000$, laminar if $Re < 2000$, and critical in between (Shashi Menon, 2015). If there is both gas and liquid in a flow, Re_L represents the Reynolds number for the liquid phase. The general equation for the Reynolds number of a liquid pipe flow is:

$$Re_L = \frac{v_L d_{pipe}}{\nu} \tag{13}$$

Which is the same as:

$$Re_L = \frac{\dot{V}_L d_h}{\nu A_{pipe}} \tag{14}$$

Where
v_L - Liquid velocity $(m\ s^{-1})$
d_{pipe} - Inner diameter of pipe $(m\ s^{-1})$
ν - Kinematic viscosity of liquid $(m^2\ s^{-1})$
$\dot{V}_L$ - Volume flow of liquid $(m^3\ s^{-1})$
A_{pipe} - Internal cross-sectional area of the pipe $(m^2\ s^{-1})$
d_h - Hydraulic diameter of the pipe (m)

The kinematic viscosity, ν of the liquid is the relation between the dynamic viscosity, μ, and the density, ρ, of the liquid.

$$\nu = \frac{\mu}{\rho} \tag{15}$$

μ is only dependant on temperature (Engineering ToolBox, 2004), and since ρ only varies a tiny amount with different pressures, the kinematic viscosity remains about the same in the range of 10 to 30 bar.

The Schmidt number, Sc, is a dimensionless number which is a ratio of the momentum and mass diffusivities (Incropera et al., 2013).

$$Sc = \frac{\nu}{D_{AB}} \tag{16}$$

3.4 Gas-liquid flow behaviour

3.4.1 Bubble size

The size of CO_2 bubbles in liquid can range from micro- and milliscale to even larger. According to Bang et al. (2015), the smallest bubbles can have a diameter of some tens

of micrometers, these are called microbubbles. Jones et al. (1998) say that 580 μm is the maximum diameter in the cycle of bubble production related to carbonated water, while Barker et al. (2002) found that bubbles in carbonated beverages can be up to 3.58 mm in diameter. The bubble size may vary depending on if the liquid is moving, how good the mixing is, temperature, pressure, etc. A decrease in bubble size can increase the solubility because the tiniest microbubbles have a higher surface tension, which allows the gas concentration in a liquid to remain higher for longer (Bang et al., 2015).

Mass transfer happens in the contact area between the bubble surface and the liquid. The contact area between the CO_2 bubbles and the water is determined by the size and geometry of the bubbles when they are being mixed into the liquid. Depending on the turbulence, inclination of the pipe, mixing tee efficiency etc., the behaviour of the bubbles may vary.

Bubbles will always tend to a spherical form because the surface tension is forcing towards the most volume per surface area. However, bubbles may not be able to achieve a fully spherical shape while flowing in a pipe. In fact, there are several types of flow patterns that can occur in two-phase horizontal flow, as seen in Fig. 3.

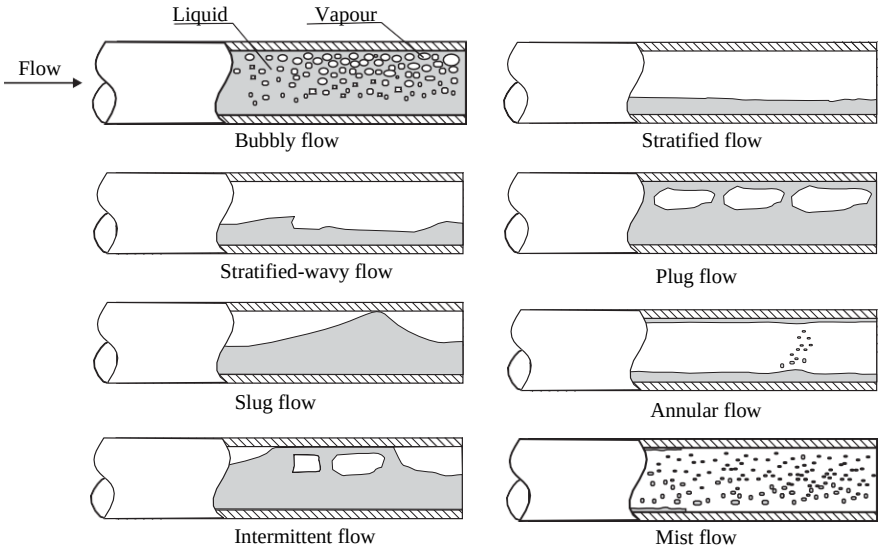

Figure 3: Two-phase flow patterns in horizontal flow (Moreno Quibén, 2005).

Which flow pattern that occurs, depends on the superficial velocity of both fluids. Moreno Quibén (2005) listed several different flow regime maps for horizontal pipe flow. Fig. 4a is a flow regime map based on the findings from Baker (1953), while Fig. 4b was originally presented in Mandhane et al. (1974). It is clear from both Fig. 4a and Fig. 4b that if there is high superficial liquid velocity and low superficial vapour velocity, then there will most likely always be bubble flow.

If it is assumed that we have spherical bubbles in a turbulent bubble flow, then the interfacial area can be approximated to the combined surface area of all the bubbles. The

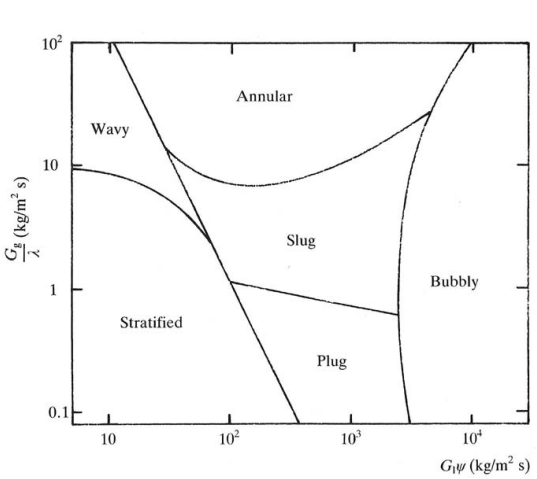

(a) The x-axis relates to the superficial liquid velocity, while the y-axis relates to the superficial gas velocity (Moreno Quibén, 2005; Baker, 1953).

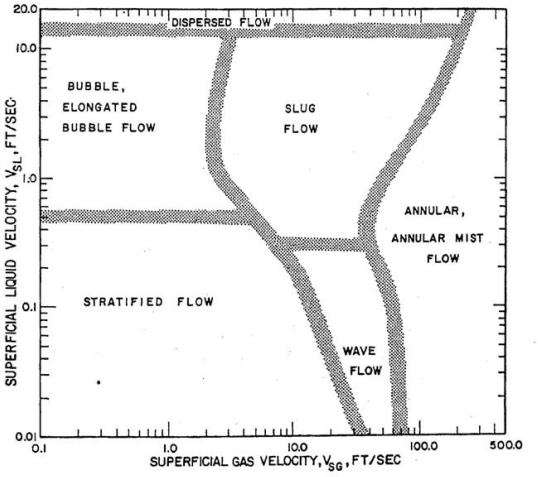

(b) The x-axis relates to the superficial gas velocity, while the y-axis relates to the superficial liquid velocity (Moreno Quibén, 2005; Mandhane et al., 1974).

Figure 4: Flow pattern maps for horizontal two-phase flow in a tube

surface area of one bubble is:

$$A_b = \pi d_b^2 \tag{17}$$

Thus, the total contact area becomes:

$$A_{interface} = \sum_{i}^{N_b} A_{b,i} \tag{18}$$

Where N_b is the number of bubbles. This sum adds together the surface area of every single bubble, but then there will be a need to know every single bubble diameter. A simplified model may assume that all bubbles have the same diameter. Then the interfacial area can be expressed directly by the total volume of gas and the bubble diameter:

$$A_{interface} = N_b A_b = \frac{V_{CO_2}}{V_b} A_b = 12 \frac{V_{CO_2}}{d_b} \tag{19}$$

This expression is reached by using the fact that with identical bubbles we have $N_b = \frac{V_{CO_2}}{V_b}$, where:
V_{CO_2} – Volume of CO_2 gas (m^3)
V_b – Volume of one bubble, $\frac{\pi d_b^3}{12}$ (m^3)

3.4.2 Mixing

CO_2 gas bubbles have less density than water, so a rising effect will naturally happen in still water because of buoyancy. In laminar bubble flow the effect is also present, so the bubbles will rise to the top of the pipe. This may result in bigger bubbles or elongated

bubble flow, which turns to inefficient use of CO_2 area and the available water. Therefore, it may be better for the mass transfer to have a turbulent flow so that the turbulence both distributes the bubbles on the whole cross-section and also breaks up the bubbles into smaller bubbles.

It must be considered what other effects the turbulence may create. When you shake a can of soda, bubbles appear more rapidly, meaning that CO_2 is released from the beverage quicker than if it was still. This is because "the bubbles formed by turbulence provide an easier way for the dissolved gas to escape" (Scientific America). This is however not directly comparable to an offshore system for carbonated water injection that is kept at high pressure. As Høgli (2020) mentions in his thesis, turbulent flow is of highest interest because the water injection is already happening at a turbulent state. Still, it is always interesting to perform experiments with other types of flow, since the results may not necessarily be as expected and could show new possibilities.

For the CO_2 and H_2O streams to be mixed, we need a mixer. In this thesis, the term *mixer* is used for something that sends CO_2 in contact with the water. Therefore, it can be something as simple as a tee mixer, which is just a T-shaped pipe fitting with two inlets and one outlet. This is a very cheap and easy installment for mixing together the two streams.

Mixers can be configured in many different ways, either with moving or static mixing elements, and with different angles between the joining pipes. The main purpose of a mixer is combining the flows, but a good mixer can make for better mass transfer, however these types can also be expensive.

With a standard tee mixer like the one in Fig. 5, the different phases will be mixed because CO_2 is injected perpendicular to the water, which leads to a change in gas flow direction and the gas is dispersed in the liquid because of turbulence. Tee mixers are not considered the best, but they are cheap and are believed to serve the purpose of this project because of high water flow (Høgli, 2020). A high water flow makes the flow turbulent, which will break up the gas bubbles and help with the mixing.

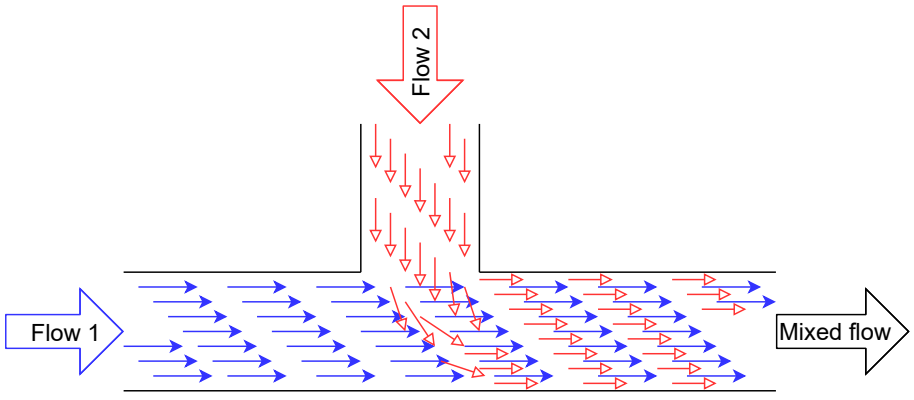

Figure 5: Simple sketch of a tee mixer

In their mixing tee design correlations study, Cozewith and Busko (1989) found that the mixing length, L/D, is proportional to the square of the ratio between branch stream

and main stream diameter, $(d/D)^2$. In addition they found that L/D was independent of Reynolds number when $Re >= 10\ 000$, and that an angle between the streams of 45° pointed upstream gave more rapid mixing than a regular 90° tee. Høgli (2020) also mentions that shorter mixing lengths might be achieved by having a 45° angled joint instead of 90° between the two streams, and also by switching streams so that the gas stream is the main stream, but these options are not included in the scope of this thesis. There are numerous other ways of creating a more efficient mixer. Static mixers from companies like Sulzer are mixing elements with some geometry inside that can be installed after a regular tee mixer. A static mixer efficiently disperses the flow around motionless mixer parts, but will add a small pressure drop (Sulzer, 2021).

Forney and Gray (1990) studied the optimal design of a tee mixer for fast reactions, and found results that could be applied on the experimental rig used in this thesis. However, they assumed that the fluids to be mixed are of the same phase and are miscible. This means that the conclusions are not necessarily the same when dealing with two phases. They found that a geometrically centered jet seemed useful if the measurement point was at distances x far from the injection point or $15 < x/D < 120$. Another conclusion was that increasing the momentum of the side tee so that the secondary fluid impinges on the opposite wall of the pipe is effective.

Calculation of mix density is important for comparison with experimental results. If there were no dissolution, then the gas would remain in gaseous phase the entire time and the density would drop because gases have lower density than liquids. However, CO_2 does have the ability to dissolve in water, which in fact causes the density to increase (Sohrabi et al., 2011).

For the overall mix density to increase, there must be no significant amount of gas left.

Assuming that the volume of the liquid phase is constant as CO_2 dissolves into it, an easy equation can be used to calculate the density of carbonated water:

$$\rho_{CW} = c_{\mathrm{CO_2}} M_{\mathrm{CO_2}} + \rho_{\mathrm{H_2O}} \tag{20}$$

In Eq. (20), the mass of all the dissolved CO_2 molecules per cubic meter of water is added to the density of the water. This is only the density of fully dissolved carbonated water, where it is assumed that the dissolved CO_2 takes up no space.

The mix density will also need to include the density for the gas phase if there is not full dissolution. This is done using the gas fraction ω_{gas}, which is the ratio between the gas volume and the total volume of gas and liquid. Since the carbonated water (or just water if no CO_2 has dissolved) is the only liquid, and CO_2 is assumed to be the only gas present, the equation for the mix density becomes:

$$\rho_{mix} = \rho_{\mathrm{CO_2}} \omega_{gas} + \rho_{CW}(1 - \omega_{gas}) \tag{21}$$

3.5 Upscaling

Before experimental results can be used to design an industrial setup, it is important to find a way of converting the small-scale results to something utilizable at a bigger scale.

Khokhar (2015) discusses the scale-up of water injection at constant Re in a horizontal pipe. This does not include CO_2 or carbonated water, but they mixed together two streams of different temperatures and came to some interesting results nonetheless. They scaled up the tube diameter with a factor of 4 and held Reynolds number constant, which caused the mixing length to increase with a factor of 2.46.

Dickey (2013) claims that choosing the correct parameter on which to base the scale-up can be challenging, and that picking the wrong one can lead to problems. He suggests keeping constant an important variable instead of dimensionless numbers such as the Reynolds number. The reason for this is that when scaling up you often want a set flow velocity, but in a bigger pipe the Reynolds number will change. It could therefore be better to scale while holding something like flow speed. Dickey does emphasize that the mixing effects should be tested over a range of variables because it is not obvious which approach yields the best scale-up.

4 Method

4.1 Procedure of simulation

There exists a variety of simulation tools that can be used to simulate mixing of CO_2 and water, but next to no simulators are able to represent a physical system with full accuracy. Therefore, several different methods of simulating physical and chemical properties and the system kinetics were used, mainly with the computer programs MATLAB, HYSYS, NeqSim and Excel.

The simulations used for comparison with the experimental rig results were done in MATLAB, while simulations for a full-scale case were done using HYSYS. NeqSim was used as a plug-in in MATLAB for thermodynamical properties, and Excel was needed to export HYSYS data.

4.1.1 MATLAB

All the relevant MATLAB scripts used in this thesis are attached in Appendix A.

CW (from the abbreviation of 'carbonated water') is the name of the core function made and used in this thesis. This function is called upon in many of the other scripts used, and can be read in its entirety in Appendix A.1. It uses Henry's law (Eq. (1)) together with mass transfer (Eq. (5)) to calculate properties of a H_2O-CO_2-mixture in a pipe. Henry's law is used to calculate the maximum solubility, and mass transfer equations are used to calculate how fast this maximum solubility is reached in the mixture.

The model is made so that everything happens in a pipe with set length L and diameter d as in Fig. 6. Dividing the pipe into N pipe sections of length $dx = \frac{L}{N}$, the pipe flow can be looked upon as a set of volumes called *nodes*. The script considers and follows one node that has an initial amount of CO_2 bubbles of a given size.

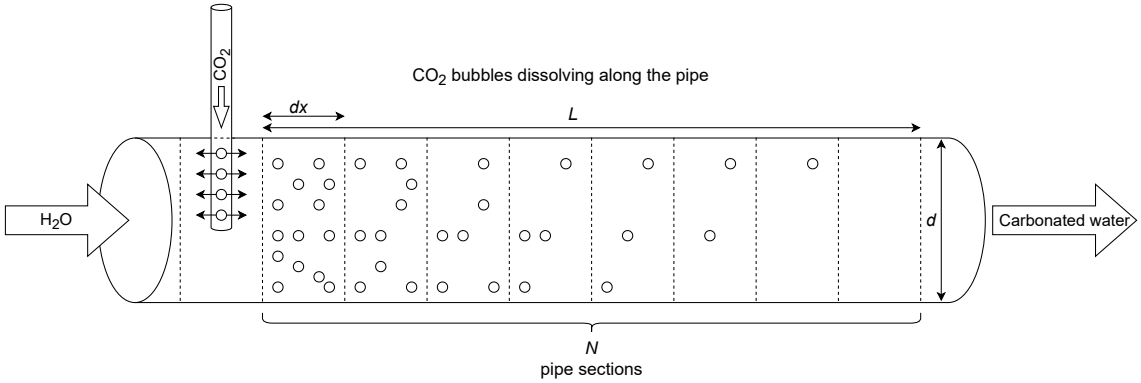

Figure 6: Simplified model of the experimental rig

When the flow speed and pipe length is known, the amount of time each node is in the pipe is also known. This residence time determines how long time the CO_2 can use to dissolve

into the water, where longer time means more dissolution. In the script, this is simplified to N iterations of mass transfer using the diffusion model with mass transfer coefficient k calculated from the script *masstrans_coeffs* in a while loop for $i < N$ and i increments for each mass transfer iteration. The maximum solubility $c_{CO_2}(sat)$ is calculated using Eq. (3) with $k^0 = 0.034$ and $\frac{d(ln\ k_H)}{d(1/T)} = 2400$ as presented in Section 3.3.1. Starting with zero aqueous CO_2 ($c_{CO_2} = 0$), the drive force $c_{CO_2}(sat) - c_{CO_2}$ is large, so the molar transfer flux n_{flux,CO_2} is large. n_{flux,CO_2} is multiplied by the total bubble surface area of the node ($A_{b,node}$) and by the residence time for one iteration step. This gives the amount of CO_2 molecules transferred. As CO_2 molecules are transferred into the aqueous phase, c_{CO_2} grows larger and the total bubble surface area in the node decreases. The next iteration step uses these new c_{CO_2} and $A_{b,node}$ values.

Put in a simple way, the mass transfer rate can be expressed by words as followed (Cussler, 2009):

$$\begin{pmatrix} rate\ of\ mass \\ transferred \end{pmatrix} = k \begin{pmatrix} interfacial \\ area \end{pmatrix} \begin{pmatrix} concentration \\ difference \end{pmatrix} \tag{22}$$

The input variables for *CW* is CO_2 mass flow, bubble diameter, pressure and a number choosing which model for k to use. Bubble diameter is assumed to be constant, which opens up for a simple way of estimating the total interfacial area, as described in Eq. (19).

The iterations stop at N iterations, which simulates that the node we have followed has reached the end of the pipe. At this point, the available information about the flow is the mix density, concentration of CO_2 in the aqueous phase, volume of CO_2 in gaseous phase and number of bubbles. It is the mix density and concentration in the aqueous phase that are of most interest, since the density can be directly compared with experimental results, and the concentration tells how close we are to equilibrium.

global_param is a function that puts out a set of global parameters that are used in *CW* and the other scripts. The function has pressure as an input argument, and temperature as a set value in the code. Pressure and temperature determine the densities of CO_2 and H_2O, which are important properties for the calculation of volume flows based on mass flows. Values for densities were gathered from WolframAlpha for a set of pressure levels. When dealing with fugacities, there was need for densities at other pressure levels than the exact ones that had been worked with previously. Instead of adding new density values for every single possible pressure level, a validity range of 10% above and below the actual pressure was added. As an example, this means that the density output for values from 90 to 110 bar give the value that is correct at 100 bar. Even though this gives an incorrect output, it was considered as a good enough simplification since the density change is not very large at these small changes in pressure.

PlotLoop is a script made to make plots using *CW*. It simply calls the function *CW* for different bubble sizes, pressure levels and mass transfer coefficients in addition to CO_2 flow which is usually the x-axis. This creates plots which presents several different scenarios that can be compared to rig results. Such comparisons are seen later in Figs. 17 to 21.

Re_k_plot was made to make a visual representation of the mass transfer coefficients, k, as a function of Reynolds number, Re. This is relevant because the different coefficients have different range of validity. Also, some of them are constant and have no specified range of validity, so this plot may help to see where it is logical to use which one of the coefficient models. This plot is seen in Fig. 15.

SolComp is a solubility comparison script, which makes a plot of solubility values from some different models, including the regular Henry's law model, a modified Henry's law model with fugacity instead of pressure, Peng-Robinson which is used in HYSYS, Diamond and Akinfiev (2003) and Duan and Sun (2003) with values from Table 3. This plot, shown later in Section 6.1, presents how similar or unsimilar the different models are, and thus how reliable they are compared to one another. Using NeqSim, fugacity coefficients for CO_2 are easily achieved at the desired pressures with the following function call

FugCoeff=system.getPhase(0).getComponent('CO2').getFugasityCoefficient()

where *system* is a system of arbitrary flow rates of CO_2 and H_2O at 303 K and a given pressure level. *getPhase(0)* represents the gas phase, which is CO_2 and a very tiny amount of water vapour. This water vapour reduces the partial pressure of CO_2 but only in a small, negligible amount. Fugacities for pressure above 50 bar were not added, since that is near the critical pressure. At supercritical state, the fugacity can't be calculated the same way in NeqSim, since CO_2 will be present not only as a gas, which was the criteria for the *getPhase(0)* function.

4.1.2 HYSYS

HYSYS is a simulator tool which can be used on chemical processes. This program is powerful and can help to simulate a full-scale CWI system. With different functions such as optimization and power calculation, there can be drawn conclusions regarding how to design an efficient real-life system. Industrial components and material streams are added to a flowchart, and properties are set by the user. For HYSYS to calculate further the system has to converge, meaning that all the necessary properties need to be set to valid values, and all connections between components need to be correct. Regulating the flows and calculating the energy consumption for multiple setup alternatives can be done at the same time. This way, a comparison of the different solutions is achieved using a simple spreadsheet.

The starting point for the simulations is CO_2 gas and liquid water at 1 atm and 18 °C, and the goal is to achieve homogenous carbonated water at a high pressure of 200 bar. A matter of interest is whether it is more efficient to do the mixing or the pressure increase first. To increase the pressure of a gas, compressors are needed. At large pressure ratios, the temperature rise can be very large, and efficiency might drop (Perez, 2011). A solution to this is to have multi-stage compressing with cooling in between. The drawback of this is the cost of more components, but the economical aspect is not discussed in this thesis.

The pressure of a liquid can be increased with the use of a pump. The pressure ratio can

be large, so there is no need for many pumps. No gas can be present in the pumps, or else HYSYS will show the error message "Vapour in inlet stream" and the system will not converge.

If mixing is done at 1 atm, then no compressors are needed, since the carbonated water can be pumped when the CO_2 is fully dissolved. If compression is done before mixing, then power is used to increase the pressure, but solubility is gained. The amount of CO_2 that can be dissolved is therefore larger.

HYSYS also has a lot of tools that can be beneficial to use for comparison with and guidance for the MATLAB simulations and the physical experiments. Using the *Case Studies* module, it's possible to run the simulation with a predetermined set of input arguments, i.e. different mass flows of CO_2 for a given range of pressure. The chosen equation of state for this HYSYS system is Peng-Robinson, which has great accuracy at predicting liquid phase densities (Peng and Robinson, 1976). Solving for mass density of the mixed stream, a plot of mix density for the ratio between CO_2 and water flow is achieved. This shows the maximum solubility, i.e. the steady-state after long reaction time. HYSYS does not take mixing efficiency or pipe length into account, so these results can only be used as a pointer for the expected maximum solubilities. However, that also means that this pointer is as much valid for a small-scale system as for a full-scale system. A plot of solubility at different pressures using Case Study is shown in Fig. 14 in Results, while Fig. 7 shows the system used to get these results. Here, the CO_2 and H_2O flows are set to the same temperature and pressure, the values of which are set in the Case Study.

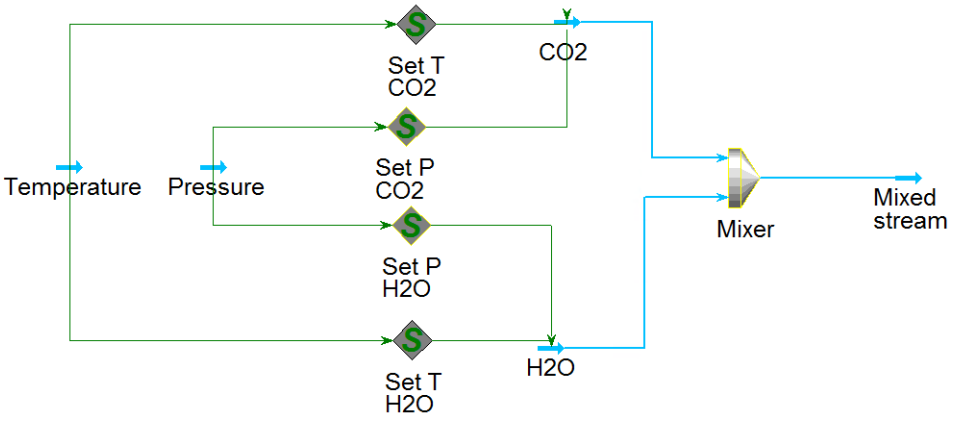

Figure 7: System used in HYSYS Case Study

4.2 Procedure of experiments

Experiments are done using the experimental rig described in Section 5.

Each set of experiments starts by setting a constant pressure and a constant rate of water. Beginning at at 0 kg/h CO_2, the flow of carbon dioxide is increased while the mixture density at the outlet is measured.

All flow streams, i.e. the CO_2 flow, water flow and mixed flow, are controlled and measured

separately using the devices shown and listed in P&ID of CW rig and Table 5. Pressure is controlled with PIC 0008, H_2O flow is controlled with FIC 0005, CO_2 flow is controlled with FIC 0012, and specific gravity (density) is measured with DI 0009.

Since the rig is brand new, there haven't been performed any experiments prior to this thesis. Therefore, it is expected that there will be some challenges in the start. After each set of experiments, there will be a discussion with the Equinor team regarding how to make the rig better, and changes to the rig or the experiment procedure are done correspondingly.

There are many factors that can be tuned and can effect the carbonation. Therefore, it is appropriate to tune one parameter at the time. Because of delays, it was not possible to perform as many experiments as originally wanted. Therefore, all experiments were done with the same pressure level. However, by changing the other parameters such as flow rate of water, pipe length and the mixing point, there are still many conclusions that can be drawn. An interesting question is for example if dissolution is better at high water flow rates because of more turbulence, or at low flow rates because of longer residence time.

5 Experimental rig

5.1 Description

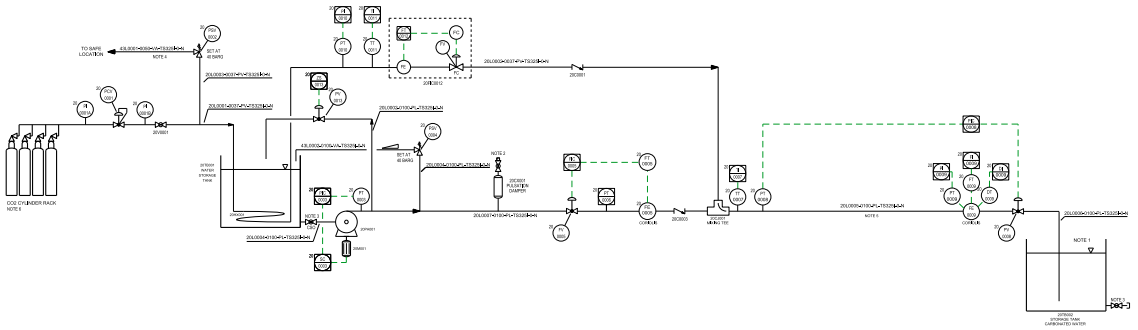

Figure 8: Piping and instrumentation diagram of the experimental rig. Complete P&ID with comments in Appendix B.

An experimental rig was constructed in 2020 at Equinor's facilities at Rotvoll in Trondheim after design by Emil Høgli as described in his master's thesis (Høgli, 2020), with some adjustments. The rig consists of a straight metal pipe connected with a tee joint to a fresh water supply and a CO_2 gas supply in one end. At the other end, a coriolis flow meter measures the density of the mixed flow. By varying the flow rate of water and CO_2, information about the solubility of CO_2 in water at pressures up to 40 bar can be found. These results are to be compared with computer simulations, and will hopefully help to make a good and reliable simulator that can be used on industrial scale. An as-built piping and instrumentation diagram of the rig is provided in Fig. 8, and a photo of the rig is seen in Fig. 9. All components are listed in Table 5.

Adjustments from Høgli's original design are, amongst others, that the installed pipe was straight instead of bent and that no electrical powered heating bath for the CO_2 stream was installed. This could result in some deviations from Høgli's computations of beneficial flow rates and corresponding outlet densities.

Throughout this project, two additional adjustments were made:

- A new mixing configuration for better mixing
- A hose attachment for longer residence time

Originally the mixing point between the CO_2 and H_2O flow consisted of a regular tee mixer as described in Section 3.4.2. The lack of a mixing element makes the mixing solely dependant on the kinetics of the flow.

After the first set of experiments it was considered necessary to make a better mixing configuration to get more efficient mixing. The CO_2 tube was extended and blocked in its end, and four holes with 2 mm diameter were drilled through both sides as shown in Fig. 10, so that the bubbles come out perpendicular to the water flow. These eight holes have a

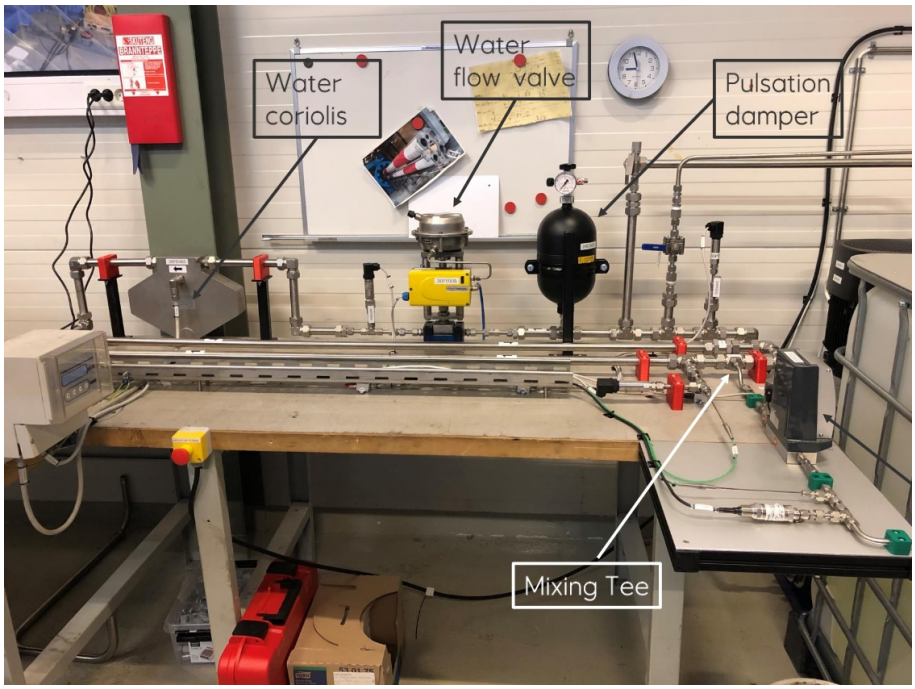

Figure 9: Picture of the carbonated water rig

combined area of 25 mm^2, which is around half of the cross-sectional area of 48.7 mm^2. That will result in a higher gas velocity which might lead to even better mixing because of greater turbulence and impingement mixing. A higher velocity in the flow direction is not wanted, because that could lead to shorter residence time which means shorter time to react with the water. However, since the gas flows through the holes perpendicular to the water flow, the velocity in flow direction should remain unchanged.

Even so, the mixing reconfiguration did not make any clear changes in the results, so it was then proposed to either make an even better mixer, or changing other factors on the rig. Since one of the problems was that we needed high flow rates to get accurate readings from the instruments, the fluids move very quickly through the pipe, thus the residence time is low. Extending the pipe where mixing is happening, the residence time also gets larger.

A 20 m long flexible hose was ordered for the purpose of control checking that the CO_2 would mix in properly if enough pipe length was available. If the original pipe was way too short, there would be a waste of time and resources to try to adjust the mixer instead of making a longer pipe. If the pipe extension is long enough that the mixture gets enough contact time, then the next step would be to adjust the more intricate variables. If the pipe extension is not long enough, the whole rig might need to be reconsidered.

The hose is a Rockmaster 2SN- EN 853 2 SN- DIM-WP type with length 20 m, outer diameter diameter 36.8 mm and inner diameter of 25.0 mm (approx. 1 inch). This means that the cross-sectional area is larger than that of the original pipe with *outer* diameter 1 inch.

(a) The new CO_2 insertion pipe

(b) Closeup of perforation

Figure 10: New CO_2 tube with blocked end and perforated sides, four holes à 2 mm on each side

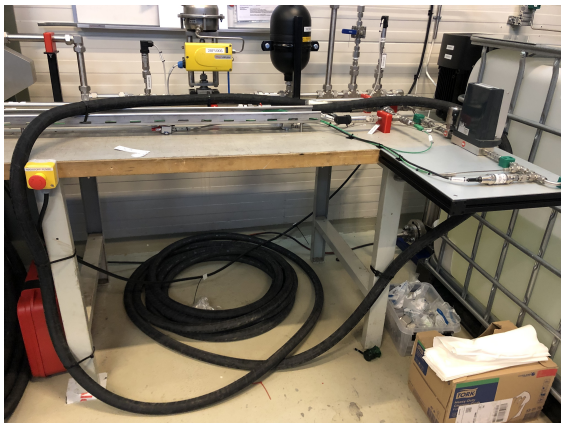

(a) Rig with hose installed

(b) Closeup of the connection point

Figure 11: Pictures of the rig after a 20 m long hose has been attached

Table 5: Components for the experimental rig with tag numbers as in P&ID of CW rig.

Component	**Description**	
20PA001 - Pump	Fluid	Water
	ΔP_{max}	48 bar
	$\dot{V}_{min}$	0.2 m^3/h
	Manufacturer	Grundfos
	Model	CRNE 1-23 Q-FGJ-T-V-HQQV
20TB001 - IBC tank - Water	Volume	1000 litres
20TB002 - IBC tank - Mixture	Volume	1000 litres
CO_2 gas bottle ×12	Fluid	CO_2
	Pressure	50 bar
	Purity	$> 99.7\%$
	Volume	600 litres (@15 °C, 50 bar)
	Manufacturer	Linde Gas
PCV0001 - Pressure reduction valve	Fluid	CO_2
	ΔP_{max}	300 bar
	$\dot{V}_{min}$	19.51 (@20 °C, 1.01325 bar)
	$\dot{V}_{max}$	252.93 (@20 °C, 1.01325 bar)
	Manufacturer	AGA Gas
	Model	SLS 250, 300 bar
20FIC0012 - Coriolis w/ control valve	Fluid	CO_2
	$\dot{m}_{min}$	2 kg/h
	$\dot{m}_{max}$	100 kg/h
	Manufacturer	Bronkhorst
	Model	M54C5I-RAD-22-Z-B
20PT0010 - Pressure sensor	Fluid	Water
	P_{max}	344 bar
	Manufacturer	Swagelok
	Model	NG5000, Model E
	Fluid	CO_2

Continued on next page

Table 5 – *Continued from previous page*

Component	**Description**	
20PSV0002 - Pressure relief valve	Diameter	4.78 mm
	Manufacturer	Gyrolok
	Model	R6000
20C0001 - Check valve	Fluid	CO_2
	Manufacturer	Swagelok
	Model	SS-CHS6-CH8
20PV0013 - Control valve	Fluid	Water
	Cv	
	Manufacturer	Flowserve
	Model	E316-003-01
20PSV0004 - Pressure relief valve	Fluid	Water
	Diameter	4.78 mm
	Manufacturer	Gyrolok
	Model	R6000
20CX001 - Pulsation damper	Fluid	Water
	Volume	3.5 litres
	Manufacturer	Hydac International
	Model	SBO250
20FV0005 - Control valve	Fluid	Water
	Cv	
	Manufacturer	Flowserve
	Model	E316-003-01
20PT0006 - Pressure sensor	Fluid	CO_2
	P_{max}	344 bar
	Manufacturer	Swagelok
	Model	NG5000, Model E
20FE0005 - Coriolis	Fluid	Water
	$\dot{m}_{min}$	25 kg/h
	$\dot{m}_{max}$	1500 kg/h

Continued on next page

Table 5 – *Continued from previous page*

Component	**Description**	
	Manufacturer	Küppers Elektromechanik
	Model	KCM 1500
	Fluid	Water
20C0003 - Check valve	Manufacturer	Swagelok
	Model	SS-CHS16-CH16
	Fluid	Water/CO_2
	Inlet diameter	1 inch
20CJ001 - Tee mixer	Inlet diameter	3/8 inch
	Outlet diameter	1 inch
	Manufacturer	Swagelok
	Model	SS-1610-3-16-6
	Fluid	Water/CO_2
20PT008 - Pressure sensor	P_{max}	344 bar
	Manufacturer	Swagelok
	Model	NG5000, Model E
	Fluid	Water/CO_2
	$\dot{m}_{min}$	25 kg/h
20FE0009 - Coriolis	$\dot{m}_{max}$	1500 kg/h
	Manufacturer	Küppers Elektromecanik
	Model	KCM 1500
	Fluid	Water/CO_2
20PV0008 - Control valve	Cv	
	Manufacturer	Flowserve
	Model	E316-003-01

5.2 Experimental uncertainty

The flow controller for CO_2 FIC 0012, is a Bronkhorst M54C5I-RAD-22-Z-B which has an operational range from 2 kg/h to 100 kg/h. Therefore, the controller is not able to be stable at low flow rates. This caused a dilemma in the operation of the rig, since high CO_2 flow was necessary to get a controlled and stable flow, but then there would be too much CO_2 in the water, and the mix density meter would either show an error message or have fluctuating measurements because of two-phase flow. So to get good mix readings, we need low CO_2 flow so that it can get dissolved, but then there is almost impossible to control or read the flow.

Figure 12: Controlling and monitoring screen of CW rig

Fig. 12 shows the monitor used when operating the CW rig. At the right hand side of the screen, there are three live plots showing the water flow rate, mix pressure and CO_2 flow rate, top to bottom respectively. The set point for water flow in this particular test was 1200 kg/h, and it is apparent that there are fluctuations between around 1182 kg/h and 1212 kg/h. The pressure is also not completely stable, fluctuating between 19.93 bar and 20.36 bar at set value of 20 bar. Neither is the CO_2 flow, which in this picture probably has had three different set values of 11 kg/h, 12 kg/h and 14 kg/h. The CO_2 fluctuations are the most severe, and impacts the density measurements.

6 Results

6.1 Comparison of solubility models

Fig. 13a shows the plot from the *SolComp* script which is described in Section 4.1.1. Five different models for CO_2 solubility in water are compared for different pressure levels at 303 K. Fig. 13b is the same figure as Fig. 13a, only zoomed in to include only 0 to 50 bar. Peng-Robinson and fugacity models were not included above 50 bar because of limitations in using HYSYS and NeqSim in the supercritical area. The fugacity coefficients found by NeqSim are as listed in Table 6.

Table 6: Fugacity coefficients for some pressure levels

$P\ (bar)$	1	5	10	20	30	40	50
f	0.9955	0.9768	0.9536	0.9080	0.8629	0.8181	0.7733

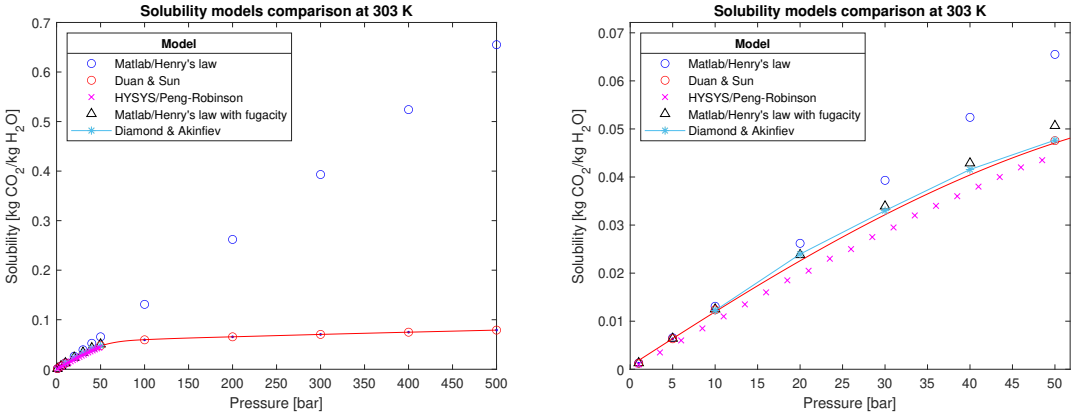

(a) 0 to 500 bar

(b) 0 to 50 bar

Figure 13: Comparison of different solubility models

The Duan & Sun values are the values from Table 3, but since there were not that many values at low pressure, a curve fit was added using the built-in fit type '*smoothingspline*' in MATLAB. The Peng-Robinson values were retrieved using HYSYS. Running the Case Study simulation described in Section 4.1.2, the values gave out Fig. 14. This plot shows the density lines, comparable to the ones in Section 6.3, so the points at which the lines start to drop are considered as the saturation points.

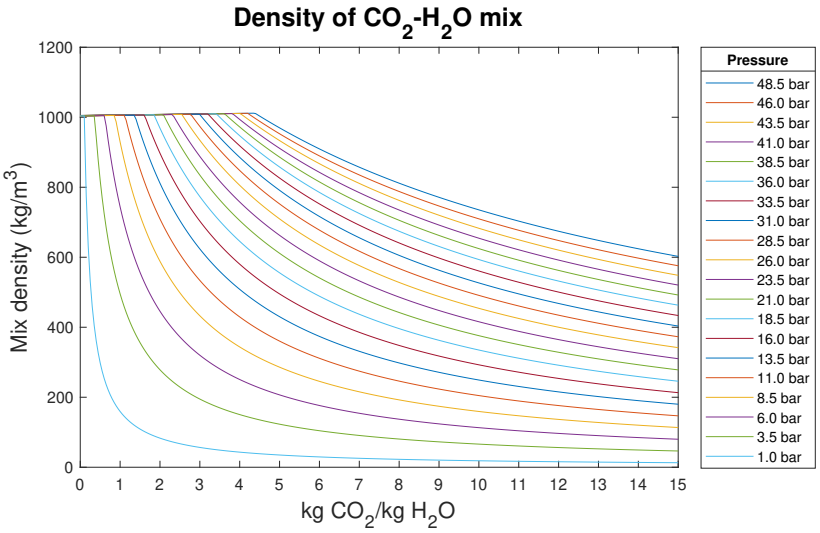

Figure 14: Results from HYSYS Case Study

6.2 Rig results

Table 7 contains all experimental data as provided from Equinor. Comments are elaborated below the table. Temperatures were only measured for the first experiment. The error message "Fault 02" has unknown meaning because of a missing manual, but the rig operators interpret it as a warning that there is too much gas / too large bubbles for an accurate measurement.

The data is listed chronologically, with the first experiments at the top. It is important to note the comments that mark where the different modifications to the rig were done.

Table 7: Results from rig experiments including comments from operators.

Set pressure ($bara$) PIC 0008	Set mass flow H_2O (kg/h) FIC 0005	Set mass flow CO_2 (kg/h) FIC 0012	**Measured specific gravity at outlet** DI 0009	Measured temperature in mix ($°C$) TI 0007
20	1200	0	1,001 [a]	-
		2	0,996	19,3
		3	0,99	18,7
		4	0,986	17,8
		6	0,974	16,3
		8	0,96	12,6
20	200	N/A	N/A [b, c]	-
	350	1,15	0,96–0,97 [d]	-
	500	1	0,98	-
20	600	0	1 [e]	-
		2	1,001	-
		3	1,001	-
		4	1,001	-
		5	1.001–1.003	-
		6	0.996–1.003	-
		7	0.990–1.003	-
		8	0.980–1.004 [d]	-
		10	0,98	-
20	1200	0	1.000–1.001	-
		7	0.994–0.999	-
		9	0.995–0.985 [f]	-
		11	0.990–0.980	-
		13	0.990–0.980 [d]	-
		15	0.990–0.980 [d]	-
20	1200	5	0.996–1.000	-
		7	0.995–0.999	-
		10	0.985–0.995	-

[a] Original setup as in P&ID (Fig. 8)
[b] All following experiments done with new mixing installment (Fig. 10)
[c] Not possible with low flow
[d] Unstable, showing *Fault 02*
[e] All following experiments done with 20 m hose installed (Fig. 11a)
[f] Here, there was also noted a measurement of the CO_2 flow of 8.9 kg/h

6.3 Simulation results

The different experiments were done with changing H_2O flow rates and pipe lengths. Therefore, a number of simulations had to be run using different initial conditions, as well as plotting with different mass transfer coefficients and bubble sizes to estimate their real values.

Different mass transfer coefficient models were plotted for their range of Re validity, see Fig. 15. Some of the k values presented in Section 3.3.2 are only valid for a specific Re value, but to make them visible in the plot, a small range was added. The exact ranges and which models are which is seen in Appendix A.3. It is *k2* that is used further in the simulations. This is the coefficient found using Eq. (11) since this has a large range of validity and has a moderately low error of 7.41%. It is also the most pessimistic one, which could fit with the not-so-impressive experimental results.

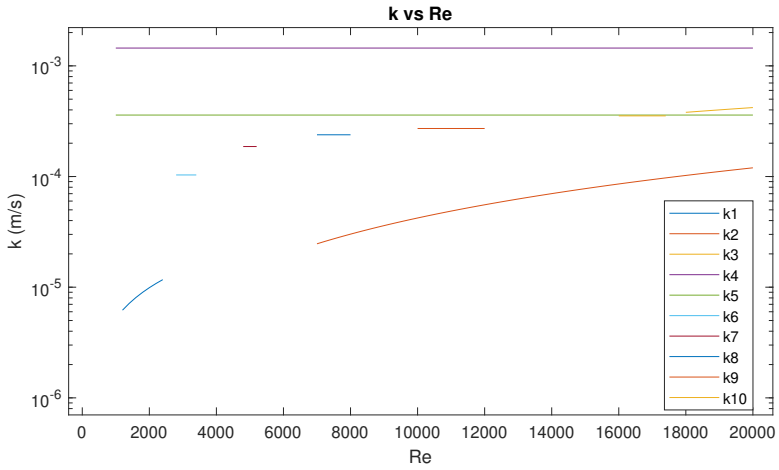

Figure 15: Mass transfer coefficients as a function of Re

The experiments were done at different H_2O flow rates, which means different Re, and therefore also different k. This makes it difficult to find a fitting way of presenting and comparing all the rig results with simulations in one plot. Rig results could be presented as a (kg CO_2/kg H_2O) vs (kg/m^3) plot, but the simulations would be complicated when including different Reynolds numbers and pipe lengths. Therefore, simulations are presented at the same H_2O flow rates and pipe lengths as the rig results that are seen in their respective plots.

With the *PlotLoop* script, each rig experiment was compared with its own simulation using as equal initial conditions as possible. This includes regulating the water flow rate, pipe length and pipe diameter. Figs. 17 to 21 are presented in the same chronological order as the experiments are in Table 7. These plots show simulations of the density at the end of the pipe, which is the same property that is measured in the rig. The different plot lines represent different bubble diameters, which are assumed to be constant through the whole pipe as described in Section 4.1.1.

Each plot line represents the density that occurs at the end of the pipe, at different CO_2

flow rates. It is therefore natural that all lines start at the density of water (when there is no gas) and end at a low density (when there is a lot of gas). Density increases as CO_2 dissolves, but at one point the density drops dramatically when there is so much gas that not enough is dissolved to increase the density. Some of the lines never increase in density, that is because very little CO_2 gets dissolved.

The smallest bubble diameter alternative is set to 10 µm, which is so small that everything that can be dissolved will be dissolved. This line will therefore have its density drop at around the saturation point, which for 20 bar is 2.62 w% according to the Henry's Law model as seen in Fig. 13b. The larger the bubble diameter, the less CO_2 is able to dissolve.

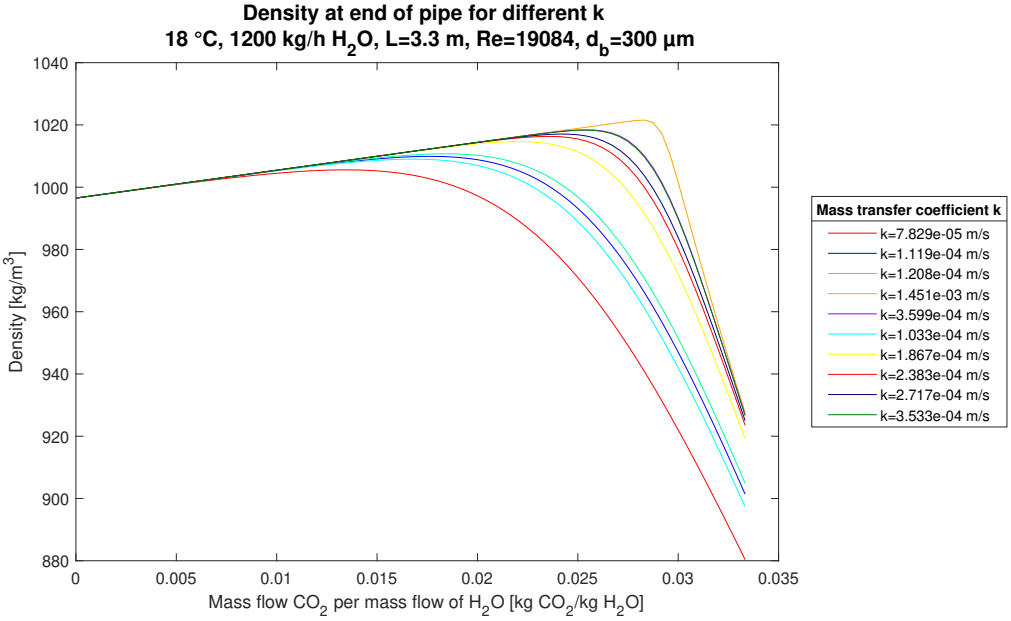

Figure 16: Effects of different mass transfer coefficients

Like bubble size, the mass transfer coefficient also has great impact on how much will be dissolved. Fig. 16 shows the effect of different k when everything else (other than CO_2 flow) is held constant. The legend shows the ten different k options in the same order as in Fig. 15. A high k gives more mass transfer and a possibility to achieve higher densities. Remember that it is the *k2* option, i.e. Eq. (11) and the second item in the legend, that is the chosen model in all the other plots.

Some of the rig measurements fluctuated between two values. These two values have been plotted for the same CO_2 rate. Rig data is visible as circles on top of the simulation lines.

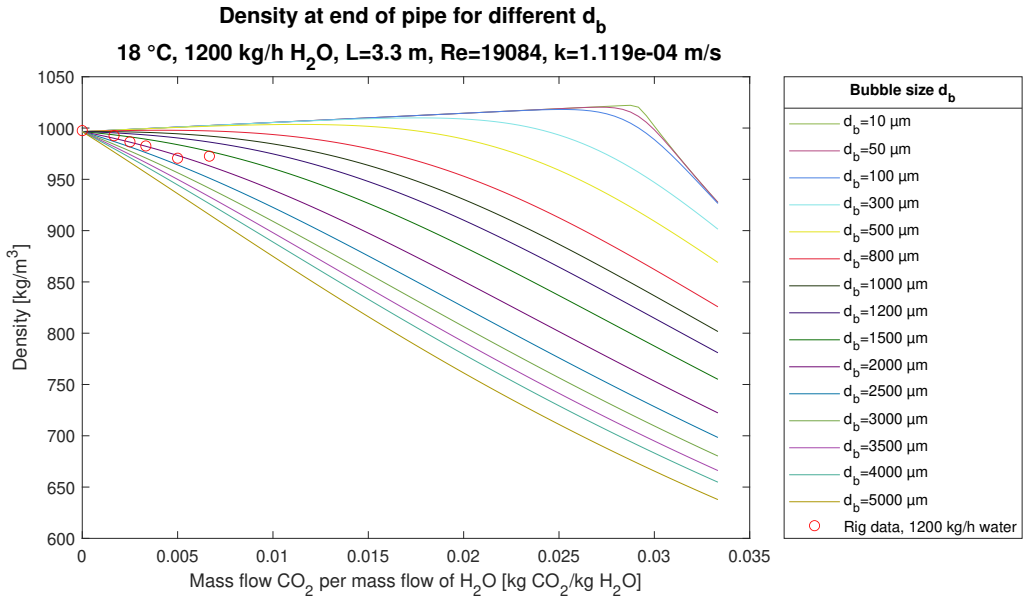

Figure 17: Simulation with results from the first rig experiment

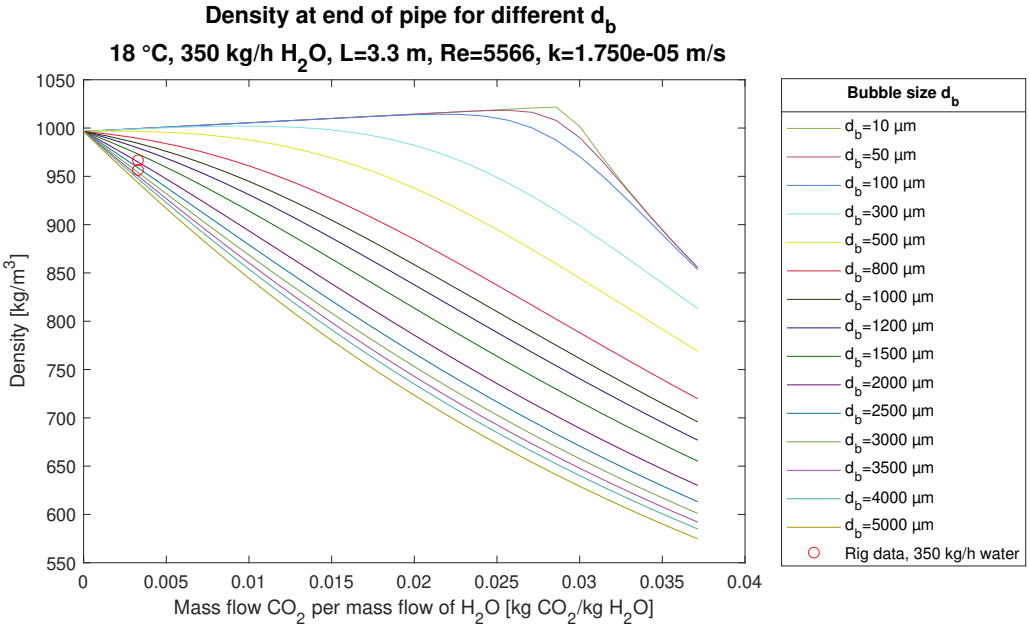

Figure 18: Simulation with results from the second rig experiment. Two data points were noted at the same flow rate, because of fluctuations between the two values.

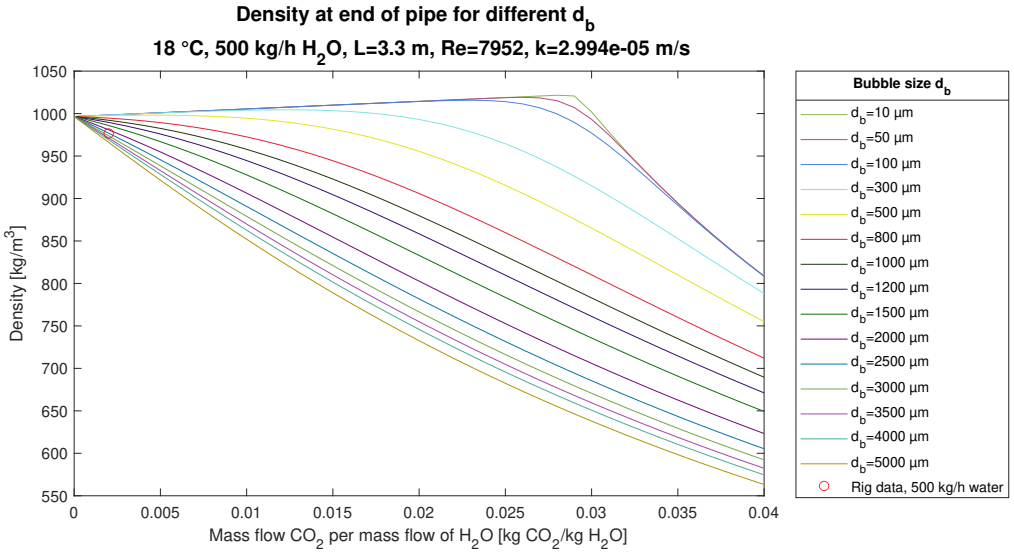

Figure 19: Simulation with results from the third rig experiment. Only one data point was noted in the experiment at 500 kg/h.

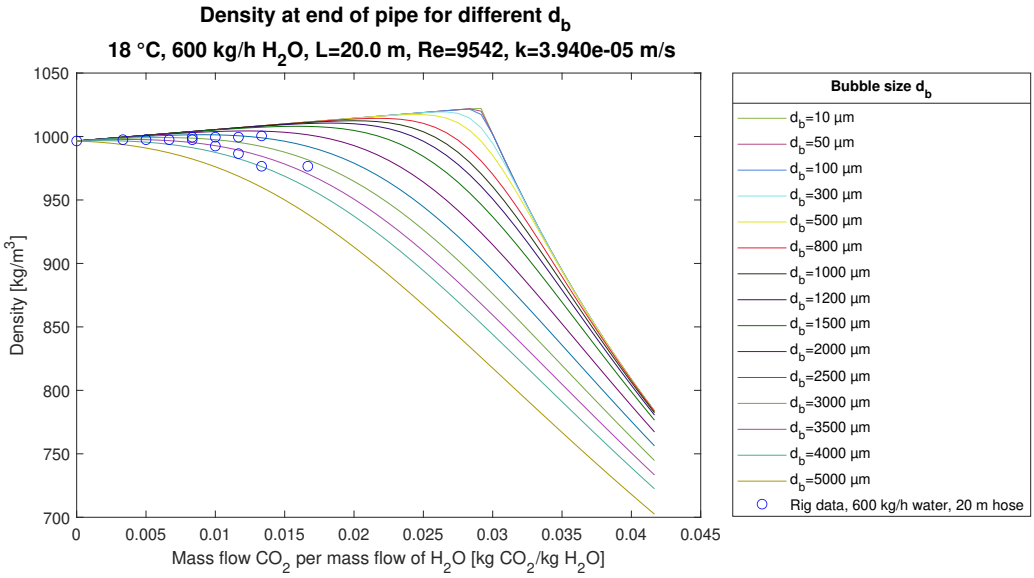

Figure 20: Simulation with results from the fourth rig experiment. The first experiment with 20 m hose installed

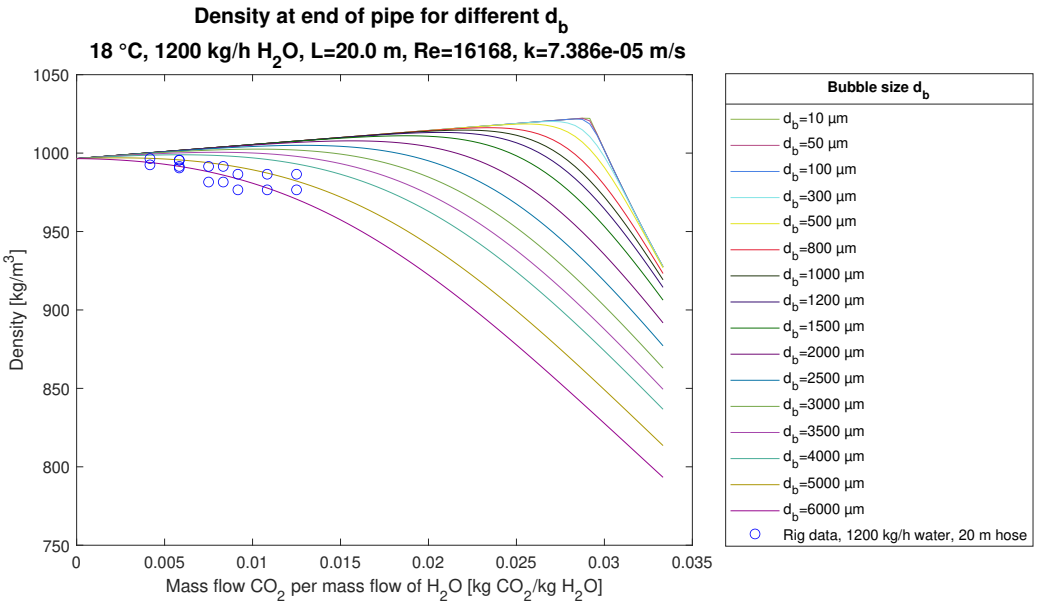

Figure 21: Simulation with results from the fifth rig experiment. Second experiment with hose, now with higher water flow

In addition to the MATLAB simulations, there were performed some simulations in HYSYS. The simulation presented now is studying the effect of dissolving the CO_2 at different pressure levels. Starting at 1 bar and ending up at 200 bar using compressors and pumps, the goal was to see how much energy usage there is per kg CO_2 dissolved. The different pressure levels for mixing became 1 bar, 3 bar, 9 bar, 27 bar, 50 bar and 200 bar which had their own separate system. The systems were copies of each other, but with an extra compressor of ratio 3 attached for each increment of pressure. This is except for the 50 bar system, where the compressor between 27 bar and 50 bar had a ratio of 1.852, or else the system would have been supercritical. The 200 bar system has a pump between 81 bar and 200 bar, because the CO_2 is at a supercritical state and can be pumped. This particular case at 200 bar needs no further pumping after mixing, but the other ones do in order to reach the goal pressure.

Between compressors, the stream was cooled to the start temperature of 300 K. The setup for the 200 bar system is shown in Fig. 22, while the other systems are similar only without the pump and with fewer compressors. All these systems were simulated with a water flow rate of 633.6 kg/h.

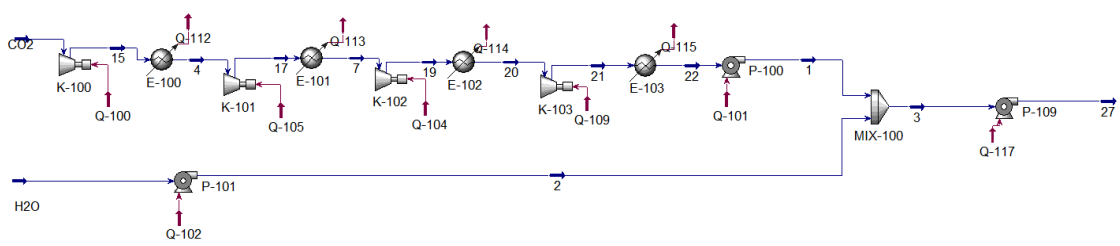

Figure 22: HYSYS system used for simulation of power consumption when making carbonated water

All the power consumptions in their respective systems were summed and compared to the maximum amount of CO_2 that was possible to solve in the system. These values are found in Table 8.

Table 8: Energy consumption for different cases in HYSYS

#Compressors	0	1	2	3	4	4 + one pump
Heat exchanger work (kW)	0.00	7.97e-2	0.49	2.22	10.33	7.68
Compressor work (kW)	0.00	8.52	0.49	2.07	8.82	4.70
Pump work (kW)	161.73	4.78	4.69	4.73	5.18	7.32
Sum comp+pump (kW)	161.73	4.87	5.19	6.81	14.01	12.03
CO_2 (kg/s)	9.72e-3	9.44e-4	2.72e-3	7.67e-3	2.82e-2	1.34e-2
kWh/kg CO_2	4.62	1.43	0.53	0.25	0.14	0.25

7 Discussion

7.1 HYSYS simulations

Despite lack of experience with HYSYS, working systems simulating real processes were achieved with results. Some time took to learn the program, and therefore the results were not as comprehensive as they could have been if more thought and care were put into it. Nevertheless, the results that came out do contribute to the discussion around how to make an energy efficient full-scale system.

The results in Table 8 show that the increase in solubility is more significant than the increase in power consumption when increasing the pressure. The configuration in Fig. 22 is not necessarily the best way of designing these systems, so it is conceivable that low-pressure mixing could be even better. At the same time it is possible that high-pressure mixing also could be improved compared to this system. Therefore, since these systems are made very similarly, it can be a general assumption that higher pressure can be beneficial for more efficient mixing. That being said, when CO_2 turns supercritical at 73.8 bar, the solubility increases more slowly, as seen in Fig. 13a. At this point, the power consumption is more significant, so this solution comes out as one of the poorer options.

The water flow rate used in the HYSYS simulations was 633.6 kg/h, which is somewhat arbitrary and possibly way lower than what would be used in the industry, but since HYSYS operates at steady-state, this should have no impact on the efficiency. This brings us to an important remark: HYSYS doesn't take kinetics into consideration. If it was possible to look at the effects from larger or smaller pipes, changing Reynolds numbers and different flow patterns, then the simulations would be of much more interest. It is also of great interest to look at the kinetics when mixing supercritical CO_2. Supercritical CO_2 does not behave the same as gaseous CO_2, so even though the solubility only increases a tiny amount when pressure is increased in the supercritical range, the kinetics could be very different. If pumps are able to efficiently pump a mix of water and supercritical CO_2 without it being fully dissolved, then suddenly the energy consumption per kg CO_2 could be drastically lower than in the non-supercritical systems.

Obviously the energy consumption is largest for the system with most compressors, but the interesting part is comparing the energy consumption with the amount of CO_2 mixed into the water. Combining the pump and compressor work and dividing with the *maximum* amount of CO_2, it showed that the benefit of pressure increase is large enough so that more CO_2 can be dissolved per kWh. As mentioned earlier, the maximum amount of CO_2 should not be reached in a real case because of the risk of going over the limit and getting gas in the pumps, but the point is still that mixing at high pressure where the solubility is higher may provide a more power efficient solution.

7.2 Comparison of MATLAB simulations and experiments

The rig results in Table 7 showed that there seems to be no significant formation of carbonated water at the conditions tested. Density drop happens rather immediately, even though the flow rates are only a small fraction of the maximum soluble amount of CO_2. The theory from the team at Equinor is that the gas needs better mixing or longer mixing length.

The simulations of the first experiment showed that the Reynolds number was as high as 19084, meaning it was very turbulent. The residence time was approximately 3.5 s based on the mass flow of 1200 kg/h. The simulation model suggests that the average bubble size is around 2000 μm, as the rig data follows this line in Fig. 17.

With flow of 350 kg/h and 500 kg/h the residence times were 12 s and 8.4 s, respectively. Even though this is long time for the reactions to happen, the results were poor, or more accurately – they were few. Only two data points in Fig. 18 and one in Fig. 19 is not enough to draw any conclusions regarding bubble size, but at least it is clear that it is challenging to dissolve CO_2 at these conditions. It must be remembered that with a low water flow, there is also a lower quantity of CO_2 that can be held in it. This, combined with the CO_2 flow controller that has a lower limit of 2 kg/h, and coriolis flow meters that are unstable, these experiments become unreliable. The simulation in Fig. 18 was done at Re=5566, which is outside of the validity range of the k model that was used (Eq. (11)). The resulting k becomes inaccurate and possibly too small. Anyhow, the rig data at the same conditions were not good enough to conclude anything regarding either k or d_b.

In the last two experiments, the 20 m long hose was used, which is over 6 times as long as the original mixing pipe of 3.3 m. In addition, the hose is 18% larger in diameter, which together adds up to a residence time 8.4 times longer than in the original pipe when running the same flow rate.

Fig. 20 shows the most promising result from all the experiments. There were unstable measurements, but if we look at the plot with optimistic eyes, there was in fact a rise in density. Severe fluctuations make it difficult to know what value the density really had, but both the lower and higher limit should be considered. With pessimistic eyes, the bubble size is at around 3500 μm, which is much larger than in the first experiment. Is it the higher values that are more correct, then the bubbles may have a bubble size of around 2500 μm, which is still larger than the first results. This could be because of less turbulence. The reason that we despite of larger bubbles get more dissolution is most likely that the residence time here was 58.9 s, so the bubbles get significantly more time to dissolve. The density fluctuations could be a result of instability in the measuring device, instability in the CO_2 flow control (as seen previously in Fig. 12), or a combination of the two.

The final experiment was done with double flow rate of experiment four. That means half the residence time, i.e. 29.4 s. These data points were also fluctuating, but not as dramatically as in the previous plot. In Fig. 21 we can see that the rig values correspond to a bubble size of approximately 6000 μm, which is larger than what has been recorded

at lower turbulence. This reveals that the simulation is flawed in the sense that there should be no reason why the bubble size should get bigger with larger turbulence. There should however be a reason to expect poorer dissolution because of lower residence time, which could be what happened.

The CO_2 flow controller is dimensioned for flows rates above 2 kg/h, but was unstable below 4 kg/h. To get reliable data, the flows therefore had to be above 4 kg/h. Simultaneously, the coriolis flow meter for the mixed flow had poor functionality when the flow was two-phase. When the mixing was so bad that almost no CO_2 was dissolved, no clear results were able to be made, since we would have needed a much lower and stable CO_2 flow to achieve one-phase carbonated water. In practice, this meant that it was difficult to get any good data neither with low water flow rates because of CO_2 rates reaching early up towards the saturation values, nor with high flows because of very low residence time in such a short mixing pipe. It was clear early that the experimental rig was not optimal.

The rig operators hypothesized that the poor solubility was due to poor mixing, since the original mixing configuration was only a simple tee. A meeting was thus held March 8 2021 with Equinor staff to discuss how to achieve better mixing. Several suggestions came, including: installing a static mixer from Sulzer; moving the tee further upstream to a point before a bend; inserting the gas pipe halfway into the water pipe; and inserting the gas pipe and making a perforated opening. Ordering a static mixer would take some time, while inserting the gas tube further inside the pipe was considered doable. The meeting concluded with inserting the gas pipe into the water pipe and blocking the end while drilling some holes in the sides so that bubbles would come out radially and hopefully result in a better mixing than in the original configuration. The new mixing point was described in Section 5.

7.3 Upscaling

As mentioned in Section 3.5, Khokhar (2015) researched the scale-up of horizontal pipe flow. Their conclusion was that "heat transfer due to mixing of both streams is achieved earlier in bigger diameters". This is a promising conclusion if the same results are true for carbonated water. It is mentioned that their problem was solved by developing empirical design equations specifically customized for their need, but that new technology could make it easier to simulate and modify the process.

HYSYS is indeed an advanced simulating tool, but it lacks the very important kinetic aspect for estimating necessary pipe lengths and diameters. A hope for the experiments was that they could provide a reliable set of data where it was possible to find a fitting relation for mass transfer coefficient and bubble behaviour at these types of conditions. This did not work out as planned because of delays and problems with the rig. The few results we got, combined with the results in Table 8 suggests that a possible step towards the design of a full-size system is to use compressors to compress the CO_2 close to, but not above, the critical pressure and have a moderate flow rate. These two factors ensures that the solubility, turbulence and residence time is high. How to pinpoint the exact values

requires further research.

From Table 3, we get the solubility of CO_2 in water with 4 m salinity, which is a little bit above the average salt level of 3.5% in regular seawater (McGill University, 2007). For the scale-up case described in Section 2, we are interested in knowing how much water is needed to safely store 180 000 tCO_2 per annum. We also want to estimate a required pipe length. Since there will be no discussion of pump efficiency here, we will look at mixing at 200 bar and 300 bar. With the results from the experimental rig in mind, it is challenging to reach CO_2 values near saturation. Let's assume that 50% of maximum solubility is a fair amount of CO_2 that can reliably be dissolved without problem in a full-scale case, and that we need a residence time of 1 minute, similar to experiment 4. To give an example for a pipe length, we assume that the mixing pipe diameter is 1 m. The assumptions for the case and the results that they give through simple calculations are presented in Table 9.

Table 9: Scale-up case

Assumptions	
CO_2 flow	180 000 t/year
Solubility @200 bar, 4 m	0.6849 mol CO_2/kg water
Solubility @300 bar, 4 m	0.7515 mol CO_2/kg water
Molar weight CO_2	44.01 g/mol
Max amount CO_2	50% of saturation level
Residence time	60 s
Pipe diameter	1 m
Kinematic viscosity water @30 °C	$0.8{\cdot}10^{-6}$ m^2/s
Results	
Water flow rate @200 bar	1363.39 m^3/h
Water flow rate @300 bar	1242.56 m^3/h
Pipe length @200 bar	28.9 m
Pipe length @300 bar	26.4 m
Re @200 bar	602 750
Re @300 bar	549 333

If we were to hold the Re constant at 10 000 like in experiment 4 instead of setting a pipe diameter, the pipe *diameter* would end up at around *60 m*. This is ridiculously large, which shows that it can be crucial to pick the wrong holding parameter, just as Dickey (2013) postulated.

8 Further work

The experimental rig at Equinor has needed some adjustments, but it is starting to give out results. More tests should be done at different flow rates and with different pipe lengths. There has been ordered a 10 m long hose in addition to the 20 m hose already installed, and it should be possible to connect the two hoses to get a 30 m long mixing tube. Redoing experiment 4 (Fig. 20) and 5 (Fig. 21) with an even longer pipe would tell what effect the pipe length and thus also residence time has.

A suggestion that came up at a meeting with Equinor was to install a pump at the end of the pipe and look at pump efficiency instead of mix density since a pump would require more power if there is gas in the mix, because of the compressibility.

It is also worth considering investing in a good static mixer element. This could be a very relevant matter of interest if it shows that installing such a component can cut down on the pipe cost for a full size rig.

Regarding simulations, the MATLAB scripts used in this thesis are based on many simplifications, including: Henry's law being valid at higher pressures; bubble flow; identical bubbles, and that Eq. (11) is the best mass transfer coefficient model. Therefore, a model with more accuracy and more thorough examination of the different equations should be worked on.

Suggestions for design of an industrial-scale CWI system should come after more certain results give indications on what to expect when scaling up. If possible, pipes with larger diameters could be tested to look at differences when only the diameter is changed. Also, the effects from salinity both on solubility and on equipment should be investigated, since an offshore rig will use seawater.

9 Conclusion

Experiments on carbonated water were done at 20 bar pressure and ambient temperature using water flows of 300 kg/h, 500 kg/h, 600 kg/h and 1200 kg/h, with mixing lengths of 3.3 m and 20 m, measuring mix density at different CO_2 flow rates. These results were compared with simulations from MATLAB and HYSYS to find information about the unmeasurable properties in the experimental systems.

It is unknown whether it is the higher or lower density measurement that is more accurate, but it is fair to assume that the density did in fact go up in the fourth rig experiment (Fig. 20), even though it was very unstable. The results were much poorer in rig experiment number five (Fig. 21), with the only difference being higher water flow. The flow was in fact doubled, meaning half the residence time, but also higher turbulence. This suggests that at some point, the residence time is of more importance for the dissolution of CO_2 than turbulence is. Still, at 300 kg/h there were very poor results, but then again the turbulence was even lower and the pipe length was shorter. There could exist a sweet-spot where the water flow is high enough to create much turbulence but low enough to ensure long residence time.

If pipe length is a limiting factor, then there should be investigated how to make a faster dissolution. A solution to this could be to mix and disperse better so that bubble sizes shrink, or increasing the residence time. In order to have a low energy consume per kg CO_2 stored, it seems to be beneficial to mix CO_2 and H_2O at a pressure close up to the critical pressure. Above critical pressure, the benefit of increased solubility is lower, and compressing and pump work gets higher.

Bibliography

H. Ahmadi, M. Jamialahmadi, B. S. Soulgani, N. Dinarvand, and M. S. Sharafi. Experimental study and modelling on diffusion coefficient of co2 in water. *Fluid Phase Equilibria*, 523:112584, 2020. ISSN 0378-3812. doi: https://doi.org/10.1016/j.fluid.2020.112584. URL https://www.sciencedirect.com/science/article/pii/S0378381220301308.

P. W. Atkins and J. De Paula. *Atkins' Physical Chemistry*, volume 8. 2006. URL https://archive.org/details/atkinsphysicalch00pwat.

O. Baker. Design of Pipelines for the Simultaneous Flow of Oil and Gas. All Days, 10 1953. doi: 10.2118/323-G. URL https://doi.org/10.2118/323-G. SPE-323-G.

J.-H. Bang, K. Song, S. Park, C. Jeon, L. Seung Woo, and W. Kim. Effects of co2 bubble size, co2 flow rate and calcium source on the size and specific surface area of caco3 particles. *Energies*, 8:12304–12313, 10 2015. doi: 10.3390/en81012304.

G. Barker, B. Jefferson, and S. Judd. The control of bubble size in carbonated beverages. *Chemical Engineering Science*, 57(4):565 – 573, 2002. ISSN 0009-2509. doi: https://doi.org/10.1016/S0009-2509(01)00391-8. URL http://www.sciencedirect.com/science/article/pii/S0009250901003918.

G. Bisweswar, A. Al-Hamairi, and S. Jin. Carbonated water injection: an efficient eor approach. a review of fundamentals and prospects. *Journal of Petroleum Exploration and Production Technology*, 2019. doi: https://doi.org/10.1007/s13202-019-0738-2.

J. A. Bours, L. Langlois, and R. Sorell. Study of carbon dioxide hydrolysis and diffusion in four different aqueous environments, 2008.

S. P. Cadogan, G. C. Maitland, and J. P. M. Trusler. Diffusion coefficients of co2 and n2 in water at temperatures between 298.15 k and 423.15 k at pressures up to 45 mpa. *Journal of Chemical & Engineering Data*, 59(2):519–525, 2014. doi: 10.1021/je401008s. URL https://doi.org/10.1021/je401008s.

J. W. Ciborowski and R. M. Rychlicki. Mass transfer in two-phase gas-liquid wavy flow. *International Journal of Heat and Mass Transfer*, 14(9):1261 – 1274, 1971. ISSN 0017-9310. doi: https://doi.org/10.1016/0017-9310(71)90176-1. URL http://www.sciencedirect.com/science/article/pii/0017931071901761.

C. Cozewith and M. Busko. Design correlations for mixing tees. *Industrial & Engineering Chemistry Research*, 28(10):1521–1530, 1989. doi: 10.1021/ie00094a015. URL https://doi.org/10.1021/ie00094a015.

R. Crovetto. *Evaluation of Solubility Data of the System CO2-H2O from 273 K to the Critical Point of Water*. Journal of physical and chemical reference data: Reprint. American Chemical Society, 1991. URL https://books.google.no/books?id=ge0pnQEACAAJ.

E. L. Cussler. *Diffusion: Mass transfer in fluid systems*. Cambridge University Press, 3 edition, 2009. ISBN 978-0-521-87121-1.

L. Diamond and N. Akinfiev. Solubility of co2 in water from -1.5 to 100°c and from 0.1 to 100 mpa: Evaluation of literature data and thermodynamic modelling. *Fluid Phase Equilibria*, 208:265–290, 06 2003. doi: 10.1016/S0378-3812(03)00041-4.

D. S. Dickey, 2013. URL https://www.chemicalprocessing.com/articles/2013/mixer-scale-up-demands-constant-attention/.

Z. Duan and R. Sun. An improved model calculating co2 solubility in pure water and aqueous nacl solutions from 273 to 533 k and from 0 to 2000 bar. *Chemical Geology*, 193(3): 257–271, 2003. ISSN 0009-2541. doi: https://doi.org/10.1016/S0009-2541(02)00263-2. URL https://www.sciencedirect.com/science/article/pii/S0009254102002632.

Engineering ToolBox. Water - dynamic and kinematic viscosity. https://www.engineeringtoolbox.com/water-dynamic-kinematic-viscosity-d_596.html, (accessed: 09.12.2020), 2004.

Engineering ToolBox. Diffusion coefficients gases in water. https://www.engineeringtoolbox.com/diffusion-coefficients-d_1404.html, (accessed: 24.05.2021), 2008.

L. J. Forney and G. E. Gray. Optimum design of a tee mixer for fast reactions. *AIChE Journal*, 36(11):1773–1776, 1990. doi: https://doi.org/10.1002/aic.690361122. URL https://aiche.onlinelibrary.wiley.com/doi/abs/10.1002/aic.690361122.

M. J. W. Frank, J. A. M. Kuipers, and W. P. M. van Swaaij. Diffusion coefficients and viscosities of co2 + h2o, co2 + ch3oh, nh3 + h2o, and nh3 + ch3oh liquid mixtures. *Journal of Chemical & Engineering Data*, 41(2):297–302, 1996. doi: 10.1021/je950157k. URL https://doi.org/10.1021/je950157k.

Hydraulic Institute. The effects of gas & liquid mixtures on rotodynamic pumps & water hammer basics, 2015. URL https://www.pumpsandsystems.com/effects-gas-liquid-mixtures-rotodynamic-pumps-water-hammer-basics.

E. Høgli. Experimental studies for carbonated injection water. Master's thesis, NTNU, 2020.

F. P. Incropera, D. P. Dewitt, T. L. Bergman, and A. S. Lavine. *Principes of Heat and Mass Transfer*. John Wiley & Sons , Inc., 7 edition, 2013. ISBN 978-0-470-64615-1.

S. Jones, K. Galvin, G. Evans, and G. Jameson. Carbonated water: The physics of the cycle of bubble production. *Chemical Engineering Science*, 53(1):169 – 173, 1998. ISSN 0009-2509. doi: https://doi.org/10.1016/S0009-2509(97)00201-7. URL http://www.sciencedirect.com/science/article/pii/S0009250997002017.

Z. H. Khokhar. Scale-up of water injection into horizontal pipe flow at constant reynolds number. *Revista Kasmera*, 01 2015.

W. Knoche. Chemical reactions of co2 in water. In C. Bauer, G. Gros, and H. Bartels, editors, *Biophysics and Physiology of Carbon Dioxide*, pages 3–11, Berlin, Heidelberg, 1980. Springer Berlin Heidelberg. ISBN 978-3-642-67572-0.

J. C. Lamont. *Gas absorption in cocurrent turbulent bubble flow*. PhD thesis, University of British Columbia, 1966. URL https://open.library.ubc.ca/collections/ubctheses/831/items/1.0059092.

J. Mandhane, G. Gregory, and K. Aziz. A flow pattern map for gas—liquid flow in horizontal pipes. *International Journal of Multiphase Flow*, 1(4):537–553, 1974. ISSN 0301-9322. doi: https://doi.org/10.1016/0301-9322(74)90006-8. URL https://www.sciencedirect.com/science/article/pii/0301932274900068.

McGill University. Seawater, 2007. URL https://www.cs.mcgill.ca/~rwest/wikispeedia/wpcd/wp/s/Seawater.htm.

M. J. Moran, H. N. S. ad Daisie D. Boettner, and M. B. Bailey. *Principles of Engineering Thermodynamics*. John Wiley & Sons, 7 edition, 2012. ISBN 978-0-470-91801-2.

J. Moreno Quibén. Experimental and analytical study of two-phase pressure drops during evaporation in horizontal tubes. 2005. doi: 10.5075/epfl-thesis-3337.

I. L. Mostinsky. Diffusion coefficient. https://www.thermopedia.com/content/696/, (accessed 08.06.2021), 2011.

NDC Registry. https://www4.unfccc.int/sites/NDCStaging/pages/Party.aspx?party=NOR, (accessed 10.03.2021), 2020.

H. Norum and T. M. Solvang. Norske utslipp høyere enn antatt: – utrolig flaut. 2021.

Norwegian Petroleum Directorate. Water injection. https://www.npd.no/en/facts/production/improved-oil-recovery-ior/water/, (accessed: 08.06.2021), 2020.

B. Pedersen. Karbonsyre. www.snl.no/karbonsyre, (accessed: 31.05.2021), 2017.

D.-Y. Peng and D. B. Robinson. A new two-constant equation of state. *Industrial & Engineering Chemistry Fundamentals*, 15(1):59–64, 1976. doi: 10.1021/i160057a011. URL https://doi.org/10.1021/i160057a011.

R. X. Perez. Why compressor ratio matters, 2011. URL https://www.pumpsandsystems.com/why-compression-ratio-matters.

Regjeringen.no. The government launches 'longship' for carbon capture and storage in norway. https://www.regjeringen.no/en/aktuelt/the-government-launches-longship-for-carbon-capture-and-storage-in-norway/id2765288/, (accessed 10.03.2021).

R. Rzehak. Modeling of mass-transfer in bubbly flows encompassing different mechanisms. *Chemical Engineering Science*, 151:139 – 143, 2016. ISSN 0009-2509. doi: https://doi.org/10.1016/j.ces.2016.05.024. URL http://www.sciencedirect.com/science/article/pii/S000925091630272X.

P. G. Røhnebæk. Nedgang i klimagassutslippene i pandemiåret 2020. 2021. URL https://www.ssb.no/natur-og-miljo/forurensning-og-klima/statistikk/utslipp-til-luft/artikler-om-utslipp-til-luft/nedgang-i-klimagassutslippene-i-pandemiaret-2020.

R. Sander. Compilation of henry's law constants (version 4.0) for water as solvent. *Atmospheric Chemistry and Physics*, 15(8):4399–4981, 2015. doi: 10.5194/acp-15-4399-2015. URL https://acp.copernicus.org/articles/15/4399/2015/.

R. Sander. Henry's law constants. *NIST Chemistry WebBook, NIST Standard Reference Database Number 69*, 2018. doi: https://doi.org/10.18434/T4D303.

Scientific America. URL https://www.scientificamerican.com/article/why-does-a-shaken-soda-fi/.

E. Shashi Menon. Chapter five - fluid flow in pipes. In E. Shashi Menon, editor, *Transmission Pipeline Calculations and Simulations Manual*, pages 149 – 234. Gulf Professional Publishing, Boston, 2015. ISBN 978-1-85617-830-3. doi: https://doi.org/10.1016/B978-1-85617-830-3.00005-5. URL http://www.sciencedirect.com/science/article/pii/B9781856178303000055.

M. Sohrabi, M. Riazi, M. Jamiolahmady, N. Idah Kechut, S. Ireland, and G. Robertson. Carbonated water injection (cwi)–a productive way of using co2 for oil recovery and co2 storage. *Energy Procedia*, 4:2192–2199, 2011. ISSN 1876-6102. doi: https://doi.org/10.1016/j.egypro.2011.02.106. URL https://www.sciencedirect.com/science/article/pii/S1876610211003031. 10th International Conference on Greenhouse Gas Control Technologies.

Sulzer. Static mixers. https://www.sulzer.com/en/products/static-mixers, (accessed: 27.05.2021), 2021.

F. Takemura and Y. Matsumoto. Dissolution rate of spherical carbon dioxide bubbles in strong alkaline solutions. *Chemical Engineering Science*, 55(18):3907–3917, 2000. ISSN 0009-2509. doi: https://doi.org/10.1016/S0009-2509(00)00022-1. URL https://www.sciencedirect.com/science/article/pii/S0009250900000221.

J. K. T.S. Kress. Liquid phase controlled mass transfer to bubbles in cocurrent turbulent pipeline flow. *Chemical Engineering Science*, 28(10):1809 – 1823, 1973. ISSN 0009-2509. doi: https://doi.org/10.1016/0009-2509(73)85063-8. URL http://www.sciencedirect.com/science/article/pii/0009250973850638.

UiO. Diffusjon. https://www.mn.uio.no/ibv/tjenester/kunnskap/plantefys/leksikon/d/diffusjon.html, (accessed: 27.01.2021), 2020.

P. Valiorgue, M. E. Hajem, A. Vassilev, V. Botton, and H. B. Hadid. Elongated gas bubble dissolution under a turbulent liquid flow. *Chemical Engineering and Processing: Process Intensification*, 50(8):854 – 858, 2011. ISSN 0255-2701. doi: https://doi.org/10.1016/j.cep.2011.05.005. URL http://www.sciencedirect.com/science/article/pii/S0255270111001139.

Appendix

A MATLAB code

A.1 CW

```
function [answer1,answer2,answer3]=cw(mass_co2_hour,d_b_micro,P_in,kNum)
global T_in  V_h2o rho_co2 rho_h2o M_co2 A_pipe R max_pipelength d_h nu
global_param(P_in);
V_co2=mass_co2_hour/(3600*rho_co2); %[m^3/s] mass_co2_h is kg CO2/h
d_b=d_b_micro*10^-6; %Bubble diameter from µm to m.

k0_H=0.034; %[mol/(kg*bar)] From NIST/Sander
dkHdT=2400; %Temperature dependant constant [K] From NIST/Sander
k_H=k0_H*exp(dkHdT*(1/T_in-1/298.15)); %Henry's law const. for CO2 from NIST/Sander
%k_H=1/710;
y_co2=1; %Mole fraction of co2 in gas phase, assumed only co2 in gas.
P_co2=y_co2*P_in; %Partial pressure in CO2 [bar]
P_co2_Pa=P_co2*100000; %Partial pressure in CO2 [Pa]
c_aq=P_co2*k_H; %Max dissolved CO2 in water at given T and P [mol_co2/kg_water]
sol_co2=c_aq*M_co2; %[kg_co2/kg_h2o]
c_co2_sat=c_aq*rho_h2o; %Max solved CO2 in water [mol_co2/m^3_water]
c_co2=0; %Initially 0 solved CO2 in the water [mol/m^3]
A_bubble=pi*d_b^2; %Surface area of one bubble
V_bubble=pi/12*d_b^3; %Volume of one bubble
n_co2_bubble=P_co2_Pa*V_bubble/(R*T_in); %Moles of CO2 per bubble, ideal gas
Re=V_h2o*d_h/(nu*A_pipe); %Initial liquid Reynolds number
dx=0.001; %Length of each node [m]

[k1,k2,k3,k4,k5,k6,k7,k8,k9,k10]=masstransf_coeffs(d_b,Re,P_in);
kVector=[k1,k2,k3,k4,k5,k6,k7,k8,k9,k10];
k=kVector(kNum); %[m/s] Choose one of the eight coefficient alternatives.

nflux_co2=k*(c_co2_sat-c_co2);
V_co2_node=dx*A_pipe*V_co2/(V_h2o+V_co2); %Volume of CO2 in the node [m^3]
V_h2o_node=dx*A_pipe*V_h2o/(V_h2o+V_co2); %Volume of H2O in the node [m^3]
N_b_node=V_co2_node/V_bubble; %Number of bubbles in the node [-]
A_b_node=A_bubble*N_b_node; %Surface area of bubbles in the node [m^2]
v_mix=(V_h2o+V_co2)/A_pipe; %Velocity of the mix [m/s]
dt=dx/(v_mix); %Time of each integral step [s]
H2=V_h2o_node/(V_h2o_node+V_co2_node);
zerosend=round(max_pipelength/dx); %End number for zeros matrix.
result=zeros(1,zerosend); %Vector for # pipe sections, based on dx and pipelength.
```

```
i=0;
while i<max_pipelength/dx
    nflux_co2=k*(c_co2_sat-c_co2); %flux of CO2 transferred [mol/(s*m^2)]
    if nflux_co2<=0
        nflux_co2=0; %Assuring no negative transfer
    end
    n_co2_transf=nflux_co2*A_b_node*dt; %transferred mol in current step [mol]
    if n_co2_transf>V_co2_node*P_co2_Pa/(R*T_in)
        n_co2_transf=V_co2_node*P_co2_Pa/(R*T_in);
    end
    V_co2_transf=n_co2_transf*R*T_in/P_co2_Pa; %transferred volume in step [m^3]
    V_co2_node=V_co2_node-V_co2_transf; %Volume of CO2 in the node [m^3]
    if V_co2_node<=0
        V_co2_node=0;
    end
    V_h2o_node=dx*A_pipe*V_h2o/(V_h2o+V_co2); %Volume of H2O in the node [m^3]
    N_b_node=V_co2_node/V_bubble; %Number of bubbles in the node [-]
    c_co2=c_co2+n_co2_transf/(V_h2o_node); %Concentration of solved CO2 [mol/m^3]
    if c_co2>c_co2_sat
        c_co2=c_co2_sat;
    end
    n_co2_solv=c_co2*V_h2o_node; %Total mol solved CO2
    A_b_node=A_bubble*N_b_node; %Bubble surface area in node [m^2]
    frac_gas=V_co2_node/(V_co2_node+V_h2o_node); %Fraction of gas
    frac_liq=1-frac_gas; %Fraction of liquid
    rho_cw=c_co2*M_co2+rho_h2o;
    rho_end=rho_cw*frac_liq+rho_co2*frac_gas; %Density at end of pipe [kg/m^3]

    i=i+1;
    %%%%
    result(i)=rho_end; %This is where we choose what to plot.
    %%%%
    H1=H2; %Old holdup, i.e. liquid fraction [-]
    H2=V_h2o_node/(V_h2o_node+V_co2_node); %New holdup [-]
    v_mix=v_mix*H1/H2; %New velocity [m/s]
    dt=dx/(v_mix); %Time of each integral step [s]
 end
%plot([dx:dx:length(result)*dx],result); %Can plot along the pipe here
pipelength=i*dx;
answer1=result(end);
answer2=k;
answer3=Re;
end
```

A.2 global_param

```
function []=global_param()

global T_in P_in V_co2 nu D_AB U_sg d_h U_rel V_h2o rho_co2 rho_h2o M_co2 ...
M_h2o d_pipe d_sm d_b A_pipe Re Sc S_pipe R max_pipelength J_l

max_pipelength=3.3; %Length of pipe [m]
d_pipe=0.0254; %Inner diameter of pipe [m]  (1 inch)
A_pipe=pi/4*d_pipe^2; %Cross-sectional area of pipe [m^2]
S_pipe=pi*d_pipe;
d_h=4*A_pipe/S_pipe; %Hydraulic diameter
T_in=18+273.15; %Initial temperature [K]
P_in=20; %Initial pressure [bar]
%P=10: rho_co2=19.26, rho_h2o=999 .P=20: rho_co2=41.19, rho_h2o=999.5.
%P=30: rho_co2=67.04, rho_h2o=999.9
rho_co2=41.19; %kg/m^3 CO2 at T_in and P_in  (WolframAlpha)
rho_h2o=999.5; %kg/m^3 H2O at T_in and P_in  (WolframAlpha)
M_co2=44.009*10^-3; %kg/mole
M_h2o=18.015*10^-3; %kg/mole

V_co2=m_co2/rho_co2; %Volume flow of CO2 [m^3/s]
V_h2o=m_h2o/rho_h2o; %Volume flow of H2O [m^3/s]

R=8.314; %[J/(mol*K)]
mu=0.00105; %Dynamic viscosity, water [Pa*s] (WolframAlpha)
nu=mu/rho_h2o; %Kinematic viscosity [m^2/s]
Re=V_h2o*d_h/(nu*A_pipe) %Reynolds number
D_AB=2.2*10^-9; %[m^2/s] Diffusivity coefficient (for CO2 at T_in and P_in).
J_l=V_h2o/A_pipe; %Superficial velocity of water [m/s]
U_rel=0; %Relative velocity of gas [m/s]

d_b=50*10^-6; %Bubble diameter, is to be tuned [m]
d_sm=d_b; %Sauter mean diameter, valid for 0.254 - 1.27 mm
Sc=nu/D_AB; %Schmidt number
```

A.3 masstrans_coeffs

```
function [k_1,k_2,k_3,k_4,k_5,k_6,k_7,k_8,k_9,k_10]=masstransf_coeffs(d_b,Re,P_in)
%Calculating the different mass transfer coefficients

global  nu D_AB d_h U_rel d_pipe Sc J_l
global_param(P_in);

%From Sherwood number
Sh1=0.00413*Re^0.916*Sc^0.5;
Sh2=1.76e-5*Re^1.506*Sc^0.5;
Sh3=0.355*Re^0.94*Sc^0.5*d_b/d_h;

k_1=Sh1*D_AB/d_pipe; %"Sh1"
k_2=Sh2*D_AB/d_pipe; %"Sh2"
k_3=Sh3*D_AB/d_pipe; %"Sh3"
k_4=0.71*(nu*D_AB)^(0.5)/(d_h)*((J_l*d_h)/nu)^(0.69); %"Rhezak1" Large eddies
k_5=1.7*(nu*D_AB)^(0.5)/(d_h)*((J_l*d_h)/nu)^(0.46); %"Rhezak2" Small eddies
k_6=0.62/6000; %"Lamont1", Re=3140
k_7=1.12/6000; %Lamont, Re=5090
k_8=1.43/6000; %"Lamont2", Re=7630
k_9=1.63/6000; %Lamont, Re=11600
k_10=2.12/6000; %"Lamont3", Re=16800
```

A.4 PlotLoop

```
%Plotting with for-loop
clc
clear all
close all
%% General
%Must choose "result(i)=rho_end;" in CW function.
global rho_h2o m_h2o_h max_pipelength
min=0; %CO2 flow rate minimum limit
int=0.5;
maks=40; %CO2 flow rate maximum limit
P_in=20; %bar
k_num=2; %Choose which mass transfer coefficient to use
d_b_vec=[10 50 100 300 500 800 1000 1200 1500 2000 2500 3000 3500 4000 5000 6000];

rng(3)
colorvec=rand(1,length(d_b_vec)*3);

%% Calling cw function
for i=1:length(d_b_vec)
    x=[min:int:maks];
    d_b=d_b_vec(i);
    for j=1:length(x)
        [res(j),k, Re]=cw(x(j),d_b,P_in,k_num);
    end
    p(i)=plot(x/m_h2o_h,res,'color',colorvec(i:i+2));
    hold on

    %lgds{i}=sprintf('d_b=%.f µm, k=%.3e m/s',d_b,k);'
    lgds{i}=sprintf('d_b=%.f µm',d_b);

end
%%
%Do you want to plot rig data? 1 for yes, 0 for no.
PlotRigData1=0; %3.3m, 1200kg/h
PlotRigData2=0; %3.3m, 350kg/h
PlotRigData3=0; %3.3m, 500kg/h
PlotRigData4=0; %20m, 600kg/h
PlotRigData5=1; %20m, 1200kg/h
j=1;
%% Rig data
if PlotRigData1==1
    %Data from rig experiment 3.3.2021
```

```
    H2OFlow=1200; %kg/h
    SG=[1.001 0.996 0.990 0.986 0.974 0.976]; %Specific gravity
    CO2Flow=[0 2 3 4 6 8]; %kg/h
    Density=SG*rho_h2o;
    p(i+j)=plot(CO2Flow/H2OFlow,Density,'ro');
    lgds{i+j}=sprintf('Rig data, 1200 kg/h water');
    j=j+1;
end
if PlotRigData2==1
    %Data from rig experiment 19.4.2021
    H2OFlow=350; %kg/h
    SG=[0.96 0.97]; %Specific gravity
    CO2Flow=[1.15 1.15]; %kg/h
    Density=SG*rho_h2o;
    p(i+j)=plot(CO2Flow/H2OFlow,Density,'ro');
    lgds{i+j}=sprintf('Rig data, 350 kg/h water');
    j=j+1;
end
if PlotRigData3==1
    %Data from rig experiment 19.4.2021
    H2OFlow=500; %kg/h
    SG=[0.98]; %Specific gravity
    CO2Flow=[1]; %kg/h
    Density=SG*rho_h2o;
    p(i+j)=plot(CO2Flow/H2OFlow,Density,'ro');
    lgds{i+j}=sprintf('Rig data, 500 kg/h water');
    j=j+1;
end
if PlotRigData4==1
    %Data from rig experiment 26.05.2021
    H2OFlow=600; %kg/h
    SG=[1 1.001 1.001 1.001 1.001 1.003 0.996 1.003 0.990 1.003 0.980 1.004 0.98];
    CO2Flow=[0 2 3 4 5 5 6 6 7 7 8 8 10];
    Density=SG*rho_h2o;
    p(i+j)=plot(CO2Flow/H2OFlow,Density,'bo');
    lgds{i+j}=sprintf('Rig data, 600 kg/h water, 20 m hose');
    j=j+1;
end
if PlotRigData5==1
    %Data from rig experiment 01.06.2021
    H2OFlow=1200; %kg/h
    SG=[0.994 0.999 0.995 0.985 0.990 0.980 0.990 ...
     0.980 0.990 0.980 0.999 0.995 0.995 0.985 1.000 0.996];
    CO2Flow=[7 7 9 9 11 11 13 13 15 15 7 7 10 10 5 5];
```

```
    Density=SG*rho_h2o;
    p(i+j)=plot(CO2Flow/H2OFlow,Density,'bo');
    lgds{i+j}=sprintf('Rig data, 1200 kg/h water, 20 m hose');
    j=j+1;
end
%%
ShowLegend=1; %Do you want to show legend? 1 for yes, 0 for no.
%% Legends and labels
if ShowLegend==1
    lgd=legend(p,lgds(:),'Location','eastoutside');
    title(lgd,'Bubble size d_b')
end
titlestring=sprintf(['Density at end of pipe for different d_b ...
    \n 18 ' char(176) 'C, %.f kg/h H_2O, L=%.1f m, Re=%.f, k=%.3e m/s'], ...
    m_h2o_h,max_pipelength,Re,k);
title(titlestring,'FontSize',13)
xlabel('Mass flow CO_2 per mass flow of H_2O [kg CO_2/kg H_2O]')
ylabel('Density [kg/m^3]')
```

A.5 Re_k_plot

```
%Plot of k models at different values of Re
clear all
close all
clc
i=1;
start=1000;
d=200;
stop=20000;
d_b=1000*10^-6;
P_in=100;
Re=start:d:stop;

for i=1:length(Re)
    [k1,k2,k3,k4,k5,k6,k7,k8,k9,k10]=masstransf_coeffs(d_b,Re(i),P_in);
    kMatrix(i,:)=[k1,k2,k3,k4,k5,k6,k7,k8,k9,k10];
end

validMatrix=[1200,2400; 6926,43282; 18000,160000; start,stop; start,stop; ...
    2800,3500; 4700,5300; 7000,8000; 10000,12000; 16000,17500];

for i=1:size(Re,2)
    for j=1:size(validMatrix,1)
        if Re(i)<validMatrix(j,1) | Re(i)>validMatrix(j,2)
            kMatrix(i,j)=0;
            kMatrix;
        end
    end
end

for j=1:size(kMatrix,2)
   plotVec(j)=semilogy(Re,kMatrix(:,j));
   lgdVec{j}=sprintf('k%.f',j);
   hold on
end
lgd=legend(plotVec(:),lgdVec(:), 'Location','northeast');
labx=xlabel('Re');
ylabel('k (m/s)');
ax=gca;
ax.XAxis.Exponent=0;
title('k vs Re')
```

A.6 SolComp

```
%SolubilityCompare
clc
clear all
close all
%Must choose "result(i)=sol_co2;" in CW function.
%% General
global rho_h2o m_h2o_h T_in
min=0; %CO2 flow rate minimum limit
int=0.5;
maks=60; %CO2 flow rate maximum limit
P_in=20; %bar
k_num=2; %Choose which mass transfer coefficient to use
P_vec=[1 5 10 20 30 40 50 100 200 300 400 500];
rng(3)
colorvec=rand(1,length(P_vec)*3);

%% Matlab Henry's law with ideal gas
for i=1:length(P_vec)
    x=10;
    d_b=100;
    [res(i),k, Re]=cw(x,d_b,P_vec(i),k_num);
end
p(1)=plot(P_vec,res,'bo');
hold on
lgds{1}=sprintf('Matlab/Henry''s law');

%% Matlab Henry's law with fugacity
Fug_coeffs=[0.9955 0.9768 0.9536 0.9080 0.8629 0.8181 ...
    0.7733 0.5237 0.3318 0.2722 0.2478 0.2385];
Fug_vec=P_vec(1:7).*Fug_coeffs(1:7); %1:7 is up to 50 bar. ...
    %Higher than that is supercrit, meaning that the fugacity constant ...
    %of the co2 gas phase is wrong, since it's no longer only as a gas.
clear res k Re
for i=1:length(Fug_vec)
    x=10;
    d_b=100;
    [res(i),k, Re]=cw(x,d_b,Fug_vec(i),k_num);
end
p(4)=plot(P_vec(1:7),res,'k^');
hold on
lgds{4}=sprintf('Matlab/Henry''s law with fugacity');
%%
```

```
PlotDuanSun=1; %Do you want to plot Duan and Sun data? 1 for yes, 0 for no.
%% Duan and Sun table data
if PlotDuanSun==1

    P_duanandsun=[1 5 10 50 100 200 300 400 500];
    Sol_duanandsun=[0.0012584 0.0063448 0.0123596 0.0475684 0.0594484 ...
    0.0655116 0.0703516 0.074822 0.079046];
    p(2)=plot(P_duanandsun,Sol_duanandsun,'ro');
    lgds{2}=sprintf('Duan & Sun');
    hold on

    Pds=[1; 5; 10; 50; 100; 200; 300; 400; 500];
    Sds=[0.0012584; 0.0063448; 0.0123596; 0.0475684; 0.0594484; ...
    0.0655116; 0.0703516; 0.074822; 0.079046];
    load census
    f=fit(Pds,Sds,'smoothingspline');
    plot(f,Pds,Sds)
end
%%
PlotHysysData=0; %Do you want to plot Hysys data? 1 for yes, 0 for no.
%% HYSYS data
if PlotHysysData==1
    HysysSolCalc
    p(3)=plot(pressures,solubility,'mx');
    lgds{3}=sprintf('HYSYS/Peng-Robinson');
    hold on
end
%%
ShowLegend=1; %Do you want to show legend? 1 for yes, 0 for no.
%% Legends and labels
if ShowLegend==1
    lgd=legend(p,lgds(:),'Location','northwest');
    title(lgd,'Model')
end
titlestring=sprintf('Solubility models comparison at %.f K',T_in);
title(titlestring)
xlabel('Pressure [bar]')
ylabel('Solubility [kg CO_2/kg H_2O]')
```

B P&ID of CW rig

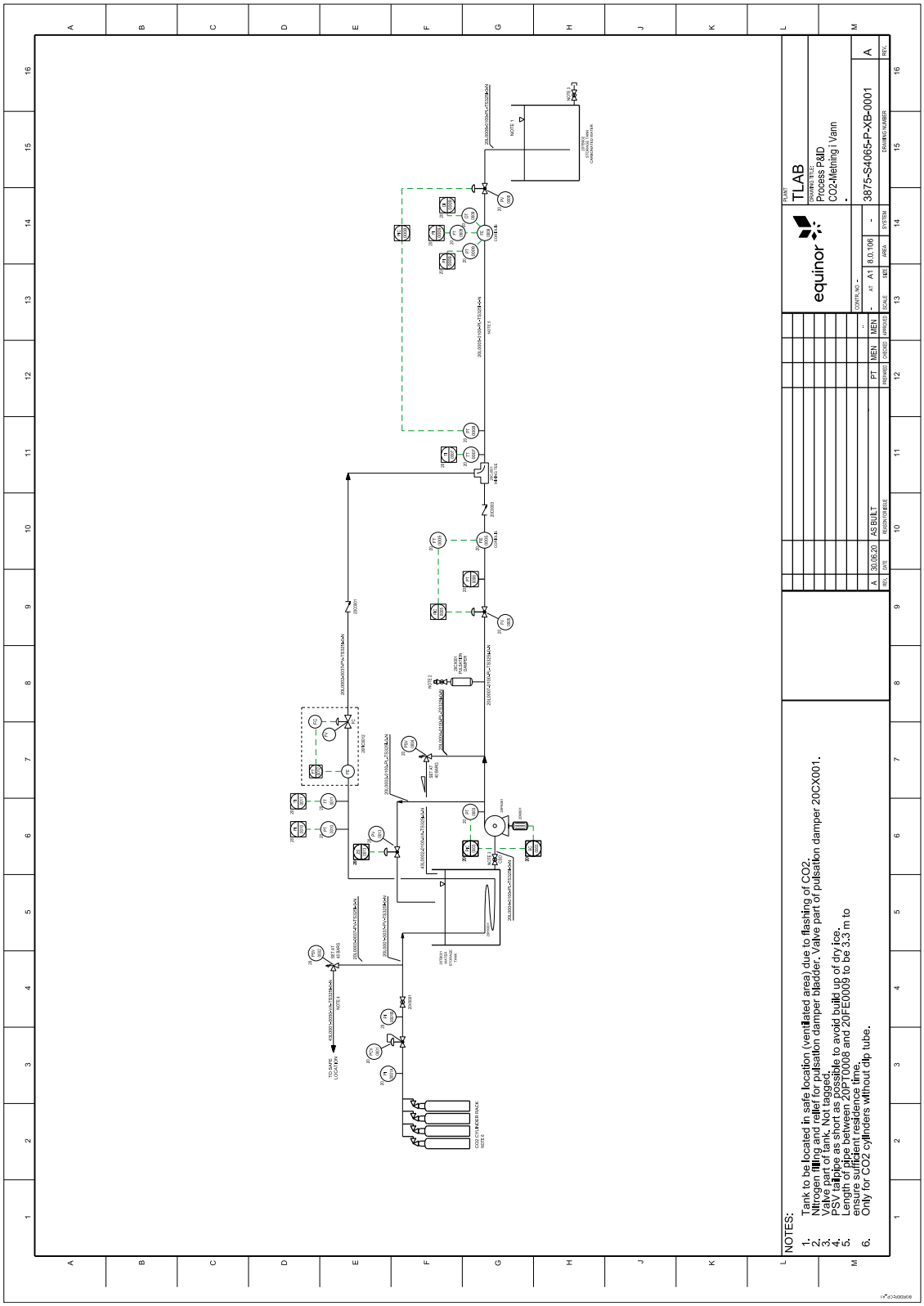

C Master's agreement

NTNU

Masteravtale/hovedoppgaveavtale

Sist oppdatert 11. november 2020

Fakultet	**Fakultet for ingeniørvitenskap**
Institutt	**Institutt for energi- og prosessteknikk**
Studieprogram	**MTENERG**
Emnekode	**TEP4900**

Studenten

Etternavn, fornavn	**Gløsen, Daniel Andreas Monsen**
Fødselsdato	**29.10.1997**
E-postadresse ved NTNU	**daglosen@stud.ntnu.no**

Tilknyttede ressurser

Veileder	**Even Solbraa**
Eventuelle medveiledere	
Eventuelle medstudenter	

Oppgaven

Oppstartsdato	**15.01.2021**
Leveringsfrist	**11.06.2021**
Oppgavens arbeidstittel	**Experimental Studies of Carbonated Injection Water**
Problembeskrivelse	**Background and objective Offshore CCS, with compact CO2 capture and CO2 disposal in injection water (carbonated water) for reservoir storage, is a technology proposed to approach zero CO2 oil and gas production in the future. Injection of carbonated water is a lower CAPEX alternative to dedicated CO2 injection well. This master thesis will focus on experimental work for efficient mixing, pumping and compressing CO2 in injection water. Scale up of the experimental data will be studied. A simplified design of a CO2 injection process will be done. Input to the design study will be provided by Equinor. The following tasks are to be considered: Review experiments and models for CO2 solubility and mass transfer in injection water Evaluation on methods for upscaling the experimental data Simulation and design of an offshore CO2 injection process Perform experimental work for carbonated injection water Test CO2 mass transfer models relevant to the experimental work**

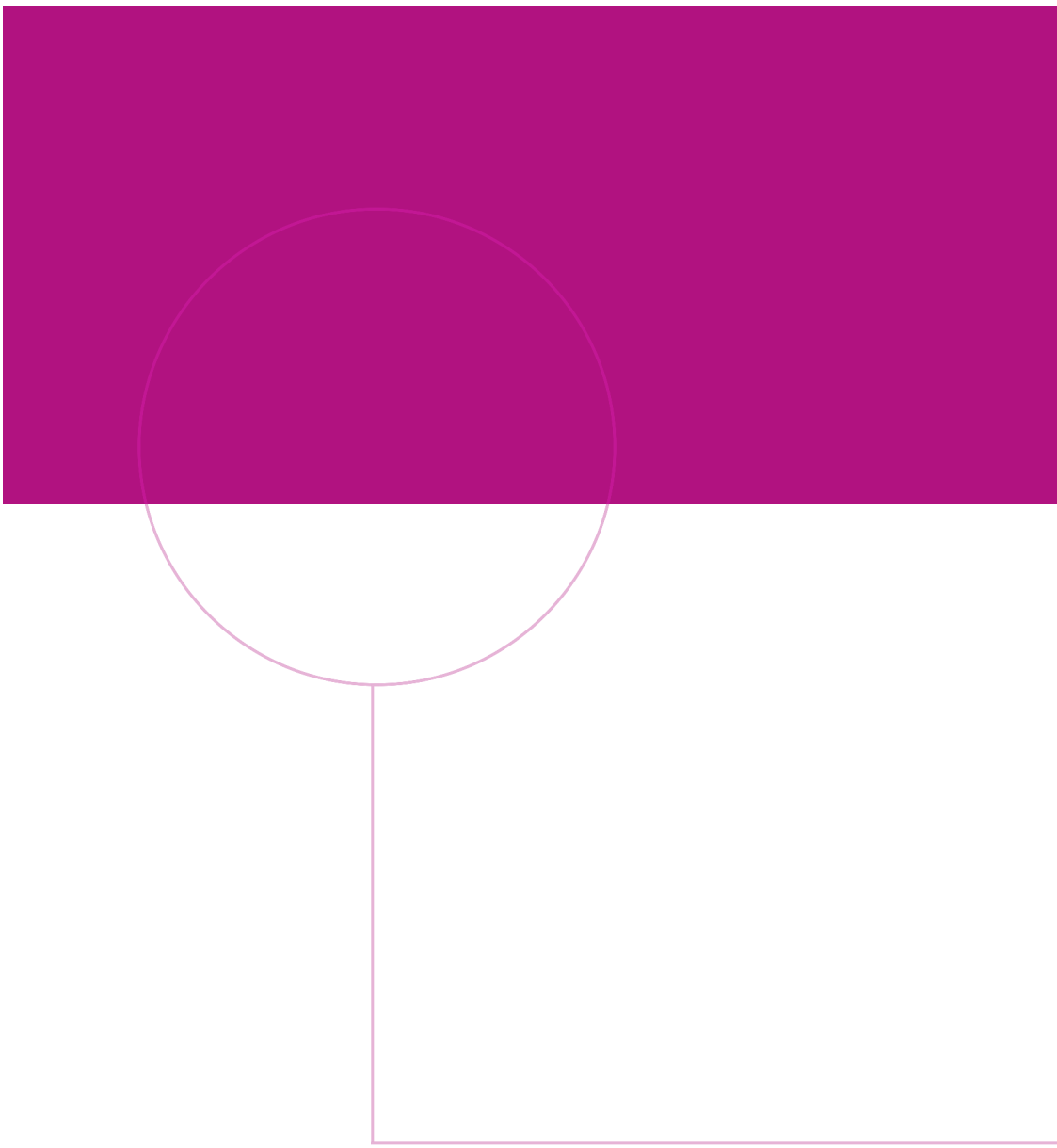

NTNU
Norwegian University of
Science and Technology

equinor